

cy 2



# **HOLOGRAPHY IN DUST EROSION FACILITIES**

**J. D. Trolinger and R. A. Belz**

**ARO, Inc.**

**September 1973**

Approved for public release; distribution unlimited.

**ARNOLD ENGINEERING DEVELOPMENT CENTER  
AIR FORCE SYSTEMS COMMAND  
ARNOLD AIR FORCE STATION, TENNESSEE**

Property of U. S. Air Force  
AEDC LIBRARY  
F40600-74-C-0001

# ***NOTICES***

When U. S. Government drawings specifications, or other data are used for any purpose other than a definitely related Government procurement operation, the Government thereby incurs no responsibility nor any obligation whatsoever, and the fact that the Government may have formulated, furnished, or in any way supplied the said drawings, specifications, or other data, is not to be regarded by implication or otherwise, or in any manner licensing the holder or any other person or corporation, or conveying any rights or permission to manufacture, use, or sell any patented invention that may in any way be related thereto.

Qualified users may obtain copies of this report from the Defense Documentation Center.

References to named commercial products in this report are not to be considered in any sense as an endorsement of the product by the United States Air Force or the Government.

HOLOGRAPHY IN DUST EROSION FACILITIES

J. D. Trolinger and R. A. Belz  
ARO, Inc.

Approved for public release; distribution unlimited.

## FOREWORD

The research reported herein was conducted by the Arnold Engineering Development Center (AEDC), Air Force Systems Command (AFSC), Arnold Air Force Station, Tennessee, under Program Element 65802F.

The results of research presented were obtained by ARO, Inc. (a subsidiary of Sverdrup & Parcel and Associates, Inc.), contract operator of AEDC. The research was conducted from July 1970 to June 1972, under ARO Project Nos. BC5016, BC5116, and BC5216, and the manuscript was presented for publication on October 18, 1972.

The authors wish to express special appreciation to the following principal contributors: J. B. Patton, Captain G. Thompson, W. R. Wimbrow, and their associates in the Propulsion Wind Tunnel Facility for their efforts in initiating the study and for their continued active support; A. E. Lennert (Technical Staff) and Major Larry Huddack and his organization at the Space and Missile Systems Organization for their early and continued support; J. E. O'Hare (Von Kármán Facility), without whose assistance the preliminary experiments in California and Washington could not have succeeded; Many Contos (Northrop Corporation), George Burghart and Dick Mayer (TRW), and George Lorenz, J. L. Harlick, and Dick Allen (Boeing Company) for their advice and assistance during key phases of the work; F. K. Hornsby and J. B. Pucket (Technical Staff) for their genius and persistence during the development of the refined system at AEDC.

This technical report has been reviewed and is approved.

JOHN R. TAYLOR  
Major, USAF  
Chief, Research and  
Development Division  
Directorate of Technology

ROBERT O. DIETZ  
Director of Technology

**ABSTRACT**

Extensive application of holographic techniques has been made in the ground test facilities at the Arnold Engineering Development Center (AEDC) for particle-field analysis and flow diagnostics. The instrumentation requirements of dust erosion facilities include a dynamic evaluation of the dust cloud, including size, number density, velocity, and distribution of dust particles. Holography has provided a unique method of performing such an evaluation. The system developed at AEDC and currently in routine use is discussed in detail. Design criteria and system capability are analyzed. It is shown that the holography system provides data which cannot be obtained with other existing instrumentation.

## CONTENTS

	<u>Page</u>
ABSTRACT . . . . .	iii
NOMENCLATURE . . . . .	viii
I. INTRODUCTION	
1.1 Optical Holography . . . . .	1
1.2 Statement of the Problem in Dust Erosion Facilities . . . . .	1
1.3 History of Holography Studies in Dust Erosion Facilities . . . . .	2
1.4 Organization of the Report . . . . .	3
II. HOLOCAMERA DESIGN	
2.1 Basic Theory . . . . .	4
2.2 Choice Between In-Line and Off-Axis Holography . .	5
2.3 Image Holography . . . . .	5
2.4 Factors That Limit the Quality of an In-Line Hologram . . . . .	8
III. MULTIPLE-EXPOSURE HOLOGRAPHY	
3.1 Basic Theory . . . . .	12
3.2 Multiple-Pulsed Lasers . . . . .	13
IV. AUXILIARY INSTRUMENTATION	
4.1 Reconstruction System . . . . .	16
4.2 Computerized Holographic Data Acquisition System .	17
4.3 Light Pulse Counter and Time Separation Electronics	18
V. IN-LINE HOLOCAMERA SYSTEMS	
5.1 Basic System . . . . .	19
5.2 AEDC Dust Erosion Facility Hologamera . . . . .	20
VI. TYPICAL EXPERIMENTAL RESULTS	
6.1 Data Taken at the Boeing and Northrop Facilities . .	21
6.2 AEDC Test Data . . . . .	22
VII. FUTURE PLANS AND REQUIREMENTS	
7.1 Fast Recording Rates (Cineholography) . . . . .	23
7.2 Automated Data Reduction . . . . .	24
VIII. CONCLUSIONS . . . . .	25
REFERENCES . . . . .	25

## APPENDIX ILLUSTRATIONS

<u>Figure</u>	<u>Page</u>
1. In-Line Hologram of a Particle Field . . . . .	29
2. Off-Axis Hologram of a Particle Field . . . . .	30
3. In-Line and Off-Axis Hologram of a Point Object . . . . .	31
4. Forming the Image with the Hologram of Fig. 3 . . . . .	32
5. Geometry for Equation (1)	
a. Hologram Formation . . . . .	33
b. Reconstruction . . . . .	34
6. Equivalent Hologram Position in Image Holography . . . . .	35
7. Collimator Image Transfer System . . . . .	35
8. Image Holography with Aberration Cancellation	
a. Producing the Hologram . . . . .	36
b. Reconstruction and Aberration Removal . . . . .	36
9. Conjugate Image Overlap Recording Condition . . . . .	37
10. Theoretical Fraunhofer Diffraction Patterns	
a. Patterns of the Intensity, $I$ , versus the Position Vector, $\rho$ , for a Fixed Particle Diameter of $160\ \mu\text{m}$ and $z = 4.1, 12.1, \text{ and } 20.2\ \text{cm}$ with $\lambda = 6328\ \text{\AA}$ . . . . .	38
b. Patterns for $z = 20\ \text{cm}$ , $\lambda = 6328\ \text{\AA}$ , and Particle Radii of $160, 80, \text{ and } 40\ \mu\text{m}$ , Respectively . . . . .	39
11. Geometry of the Particle Number Density Derivation for Hologram Recordings . . . . .	40
12. Number Density versus Diameter for Marginal and No-Hologram Recordings . . . . .	41
13. Double-Pulsed Holography of a Moving Dust Field . . . . .	42
14. Frustrated Internal Reflection Q-Switching . . . . .	43
15. Double-Barrelled, Double-Pulsing Laser Schematic . . . . .	44
16. Beam-Combining Optics . . . . .	45
17. Reconstruction Apparatus with Closed-Circuit TV . . . . .	46

<u>Figure</u>	<u>Page</u>
18. Computerized Image Analyzer	
a. Reconstruction Setup with the Computerized Image Analyzer . . . . .	47
b. Light Pen and Individual Measurement Module . . . . .	48
c. Light Pen in Use on CCTV Monitor . . . . .	48
19. Laser Light Pulse Interval Counter . . . . .	49
20. Pulse Counter and Time Interval Counter . . . . .	50
21. In-Line Image Holocamera . . . . .	51
22. Spatial Filtered Beams with Various Pinhole Sizes	
a. $d = 30 \mu\text{m}$ . . . . .	52
b. $d = 100 \mu\text{m}$ . . . . .	52
c. $d = 200 \mu\text{m}$ . . . . .	52
d. Without Pinhole ( $d = \infty$ ) . . . . .	52
23. Dust Erosion Facility Holocamera (Laser Side) . . . . .	53
24. Window Protection System . . . . .	54
25. Holograms and Images of Particles Penetrating the Bow Shock . . . . .	55
26. Sample Hologram of Model in PWT Dust Erosion Facility . . . . .	57
27. Double-Exposure Hologram of a High-Speed Dust Field and Some Reconstructions . . . . .	58
28. Velocity Spatial Distribution Curves . . . . .	59
29. Automated Hologram Analyzing System . . . . .	60
30. Conceptual Drawing of Proposed Hologram Analyzer . . . . .	61

## NOMENCLATURE

$A_o$	Amplitude of the object beam
$A_r$	Amplitude of the reference beam
$a$	Particle radius
CW	Continuous wave



d	Object diameter
I	Intensity
$J_1$	Bessel function
L	Volume depth
$L_1$	Magnifying lens in the reconstruction
M	Magnification
MHz	$10^6$ cps
N	Number density
Q	Laser cavity efficiency
S	Prism separation distance
x, y, z	Planar coordinates in the reconstruction
Z	One far-field distance
$z_i$	Reconstructed image distance
$z_o$	Object distance
$z'_o$	Distance from hologram to nearest particle in the object wave
$z_p$	Reconstruction point source distance
$z_r$	Reference point source distance
$\theta_o$	Phase distortion in the object beam
$\theta_r$	Phase distortion of the reference beam
$\lambda_1$	Recording wavelength
$\lambda_2$	Reconstruction wavelength
$\rho$	Radial coordinate on the hologram
$\rho_m$	Minimum hologram radius
$\phi_o$	Object beam phase
$\phi_r$	Reference beam phase

**SUBSCRIPTS**

i	Image
o	Object
p	Reconstruction point source
r	Reference point source

## SECTION I INTRODUCTION

### 1.1 OPTICAL HOLOGRAPHY

Holography provides a technique to record sufficient information in an optical wavefront to allow a later reconstruction or "playback" of the wave (Ref. 1). A hologram can be used like a window through which an event or scene which existed in past time can be viewed. As the size of a hologram increases, the angle of observation of a scene increases. If a hologram has surrounded an object during recording, then the holographically formed image of the object can be viewed from every angle.

An elementary requirement for producing a hologram is that light waves reflected by or passing through an object field, the object wave, be mixed coherently with a reproducible reference wave and the resulting intensity be recorded. When a hologram is illuminated by the reference wave, this wave is diffracted into separate components, one of which duplicates the original object wave.

Preliminary work in holography was started at the Arnold Engineering Development Center (AEDC) in 1967 by the Technical Staff, Experimental Research (TS/ER). During subsequent years, holography techniques have been developed for a wide variety of applications in almost every type of wind tunnel and test facility at AEDC, and these techniques now commonly provide test data which cannot be obtained by any other means. The two outstanding areas of application are in flow visualization and dynamic particle field analysis (Ref. 2). A holographic system was first applied to a dust erosion facility at AEDC in 1971.

### 1.2 STATEMENT OF THE PROBLEM IN DUST EROSION FACILITIES

A dust erosion facility simulates the aerodynamic conditions encountered by a vehicle in flight through clouds of particulate matter. In one type of facility, the dust is injected into the flow stream and is accelerated by the gas to a velocity which simulates that of the expected vehicle velocity. Other types of dust erosion facilities include those in which the dust cloud is created in an essentially stationary state and the model is passed through it, as in gun ranges and rocket sled facilities. In any of these facilities the ultimate measurement is to correlate the amount and type of erosion with the simulated conditions.

Because of nonuniformities in size and distribution of the dust under specific test conditions, the characteristics of the dust cloud at the model cannot be predicted. Accurate simulation requires that the number density, size distribution, and particle velocity and its distribution in the vicinity of the model be accurately controlled. Although the gas velocity itself may be known, the dust particles lag in velocity depending upon their size, shape, and mass. Typical dust particle diameters range from a few micrometers ( $\mu\text{m}$ ) upwards to hundreds of micrometers. Particle velocities range up to several thousand meters per second.

Optical instrumentation for studies of such particles must possess the following characteristics:

1. Time resolution less than 100 nsec to freeze motion during the data recording.
2. Space resolution preferably down to a few micrometers, and certainly better than  $30 \mu\text{m}$ .
3. A recorded volume depth extending across the test region.
4. A capability for quantitative measurement of velocity, and observation of general motion.
5. Capability of operating under ambient light conditions.
6. Capability of operating without disturbing the flow field.

Conventional photography is impractical under these conditions because the high resolution requirement placed upon this type of optical system severely limits its depth of field. Such a system can at best resolve the dust particles with a depth of field of less than 1 mm. Holography, however, satisfies all of the stated requirements and is ideally suited for this application.

### 1.3 HISTORY OF HOLOGRAPHY STUDIES IN DUST EROSION FACILITIES

In early 1970, personnel of the Propulsion Wind Tunnel Facility (PWT) encountered the problem of instrumenting a dust erosion facility for the Space and Missile Systems Organization (SAMSO) to supplement studies being conducted by the Boeing Company at the Boeing and Northrop Hypersonic Facilities. During the early planning stages of the new facility it became clear that the dust evaluation technique which had been used up to that time was not entirely suitable for SAMSO purposes. The technique utilized a mechanical catcher which, when inserted into

the flow for a period of time, collected particles for later analysis. Calibration tests indicated that supplementary or replacement methods for making analyses were needed. Holography was suggested by PWT personnel as a possible supplementary technique. Technical Staff/Experimental Research personnel evaluated the technique and concluded that it could be successfully applied. In September 1970, at the request of SAMSO, the AEDC in-line image holocamera was installed in the Northrop Hypersonic Facility in Hawthorne, California. During the following month, the same system was installed in the Boeing Hypersonic Facility in Seattle, Washington. Two holograms were made in each of 18 firings at the Northrop Facility and 15 firings at the Boeing Facility. The success of these tests proved the applicability of the holographic system. Examples of the data that were obtained are presented in Section VII.

During 1971, AEDC personnel incorporated a holographic system into the PWT Dust Erosion Facility. This system was used extensively during the calibration phases of the facility.

None of the initial systems had the capability of double pulsing (for velocity measurement) with required short pulse separation for the high-velocity particles. A newly developed double-pulsing laser which fulfilled this requirement was installed in the Dust Erosion Facility in February 1972.

The holography system is now used routinely to provide data leading to particle sizes, shapes, and velocities and the distributions of these parameters. This system, with its associated data reduction equipment, is believed to be one of the most advanced systems of its type.

#### **1.4 ORGANIZATION OF THE REPORT**

This report is confined entirely to holography in dust erosion facilities, although the requirements in many instances are clearly applicable to other three-dimensional particle fields. In Section II the discussion of holocamera design is presented, covering factors which must be considered when using holography for such applications. A brief comparison between various types of holography is made. Factors which limit the ability to produce high quality recordings are discussed. In Sections III and IV, instrumentation and special laser equipment which have been developed for producing multiple-exposure holograms and for reducing data more rapidly are described. Discussions of other

auxiliary instrumentation are also included. Sections V and VI describe the entire holocamera system and operational techniques in use at AEDC, together with typical experimental results. In Section VII, plans and requirements for future holographic systems are briefly presented.

## SECTION II HOLOCAMERA DESIGN

### 2.1 BASIC THEORY

Since the basic theory and equations for holographic recording are included in Refs. 1 and 2, only a summary is presented here. In-line holograms of a particle field are formed by passing a beam of coherent light through a volume of particles and recording the resulting wavefront. Part of the light is diffracted by the particles, and the remainder passes through the field unscattered. The unscattered (reference) light interferes with the scattered (object) light and is recorded on a photographic medium (Fig. 1). An off-axis hologram is formed by introducing a reference wave which is separate from the light passing through the object field onto the recording (Fig. 2). The laser beam is split initially in two. One portion illuminates the object field, and the other serves as the reference beam. Many geometries are suitable for off-axis holography. The object field can be illuminated directly with the laser beam or with laser light that has been diffused by a frosted glass or similar diffusing medium.

In principle, there is little difference between in-line and nondiffuse off-axis holography. In Fig. 3, if the hologram is recorded with the film at "A," it is termed an in-line (Gabor) hologram; however, if the recording is made at "B," then it is termed an off-axis (carrier frequency, sideband, or Leith-Upatnieks) hologram. This similarity does not exist when the object field is illuminated with diffuse light, since a hologram must be made with a reproducible reference wavefront.

The object wave in both cases in Fig. 3 is reconstructed by illuminating the developed recording with the reference wave as shown in Fig. 4. It is one of the components produced by the diffraction of the reconstruction wave by the hologram. If the radius of curvature, the angle of illumination, or the wavelength of the reconstruction reference wave is changed, the object wave will be altered so as to produce image magnification, a change of position of the image, and aberrations.

Equation (1) predicts the position of the reconstructed image as a function of the wavelength, radius of curvature, and position of the reference wave. (Figure 5 illustrates the geometry for Eq. (1).)

$$z_i = \left( \frac{1}{z_p} \pm \frac{\lambda_2}{\lambda_1 z_r} \mp \frac{\lambda_2}{\lambda_1 z_o} \right)^{-1}$$

$$x_i = \mp \frac{\lambda_2 z_i}{\lambda_1 z_o} x_o \pm \frac{\lambda_2 z_i}{\lambda_1 z_r} x_r + \frac{z_i}{z_p} x_p \quad (1)$$

$$y_i = \mp \frac{\lambda_2 z_i}{\lambda_1 z_o} y_o \pm \frac{\lambda_2 z_i}{\lambda_1 z_r} y_r + \frac{z_i}{z_p} y_p$$

These equations result from a first order analysis of thin holograms and are not accurate when large changes in wavelength or reference wave curvature are encountered. Under such conditions, aberrations equivalent to those of a lens result. A more general analysis is treated in Ref. 3.

## 2.2 CHOICE BETWEEN IN-LINE AND OFF-AXIS HOLOGRAPHY

In-line holography is by far the simplest type of holography and for this reason probably should be considered first in particle-field studies. However, there are many cases in which off-axis holography is applicable and in-line holography is not. Such cases exist when the particle number density or their total cross section is very large, or when the object field significantly modulates the phase of the electromagnetic radiation.

Considering practical limitations such as those typically encountered in wind tunnel facilities, including operation effects and the inability to meet all holographic requirements, in-line holography is quite satisfactory when the conditions mentioned above are not critical. (Detailed studies of these factors are included in separate reports (Refs. 4 and 5).) Since in-line holography has proven sufficient in application to dust erosion facilities, only this method will be discussed further.

## 2.3 IMAGE HOLOGRAPHY

Image holography is defined here as any type of holography in which lenses are placed between the object field and the recording. The holographic equations for image holography are identical to those for

ordinary holography if one replaces object coordinates with image coordinates and replaces reference wave coordinates with the coordinates of the reference wave point source imaged by the lens system (Ref. 6).

### 2.3.1 Imaging the Object Field Before Recording

In many practical applications one is required to place the recording equipment and instrumentation outside the test region. In some cases this places the object field at a great distance from the nearest optical element. The resolution of any imaging system (holograms included) is directly dependent upon the solid angle of radiation (scattered by the object) which can be accurately recorded. Therefore, without lenses, as the distance from the particle object increases, the area over which information must be recorded (the size of the hologram) must also increase if the same resolution is retained. This may involve more than simply increasing the physical size of the hologram, since the effective size of the hologram is determined by the ability of the film to accurately record information for later retrieval. Since the fringe contrast in the hologram is reduced at larger object-to-film distances, the physical size of the hologram may greatly exceed its effective size.

Lenses act only to transform information and are usually better optical elements than holograms are for this purpose. An alternate way of interpreting this process of imaging the object field is to consider that the lens images the holographic plate inside a wind tunnel or test chamber closer to the object field, thus improving the holographic recording (Fig. 6).

Optical elements affect the quality of a reconstruction when they do not image the object and reference beam accurately or when they introduce optical noise into the holographic recording and reconstructed image. Usually, these elements introduce less noise per square area and are capable of producing better images per square area than a hologram. The size of optical systems may limit the effective diameter of the diffraction pattern strictly by an aperturing effect. This applies also to windows or other aperturing elements placed in the recording system. The effects of a limiting aperture on the reconstructed image are presented in Ref. 7.



### 2.3.2 Choice of Lens Systems

When choosing a lens system to re-image the object field, one encounters a number of practical considerations. One of the most difficult problems in practical applications is caused by noise generated by the scattering of coherent light by dust and imperfections that may exist within the system. Therefore, the simplest type of lens system is usually the best choice for a noise-free recording. Lens aberrations must also be considered but are to be distinguished from those encountered in the holography process itself.

Basically, there are two widely used types of lens systems. The first of these is the two-collimator image transfer system shown in Fig. 7. A pair of lenses separated by the sums of their focal lengths images an object field with constant magnification. For collimated object illumination, the lens system maintains the collimated reference wave at the recording plane. Any magnification values are possible by judicious selection of lens focal lengths. The magnification of the image field is the ratio of the focal length of the second lens over the first and is independent of object position. A collimated illuminating wavefront remains collimated, a condition which is easily reproduced during the reconstruction. This configuration has relatively low spherical aberration and distortion.

The second type of imaging system uses a single lens, creating a diverging or converging reference beam. During reconstruction, the same lens is returned into the reconstruction wave, which is conjugate to the original reference wave (Fig. 8). It has been shown that images reconstructed in this manner will be free of any lens aberrations which could ordinarily be present, provided the lens orientation with respect to the film remains constant (Ref. 1). In very high resolution studies, this capability can be extremely important; however, the disadvantages of this type of lens system for use in the reconstruction system are its obvious alignment and orientation problems.

### 2.3.3 Conjugate Image Overlap

Any holographic recording reconstructs two identical (in information content) conjugate images. In direct in-line holography, these images lie on opposite sides of the holographic recording during their reconstruction (see Fig. 4). In image holography, the object field may be imaged on both sides of the hologram and therefore will reconstruct on both sides, causing an overlapping of the conjugate image fields (see

Fig. 9). This creates a position ambiguity, since one cannot distinguish conjugate images. Therefore, when one desires the spatial distribution of the data, conjugate image overlap cannot be tolerated. This problem is avoided by insuring that the imaged object field lies entirely on either side of the recording plane.

## 2.4 FACTORS THAT LIMIT THE QUALITY OF AN IN-LINE HOLOGRAM

There are a number of factors which limit the quality and resolution of an in-line hologram. Object characteristics such as size and distance from the film, the quality and geometry of the reconstruction system, and optical noise in the system during either recording or reconstruction govern the amount of useful information recorded. A system can be designed so that the last factor, noise, limits the achievable resolution of the holographic measurements. Noise may be introduced by the optical system, the recording medium, the laser, or the object field itself.

### 2.4.1 Object Distance and Size

Consider a single circular opaque particle (disk) of diameter  $D$  a distance  $z$  from the film, illuminated with collimated light. As  $z$  increases and/or as  $D$  decreases, the required effective size of a hologram of the particle must be increased to maintain image resolution -- that is, to record the same object information. A result of this is that the reconstructed image quality decreases as  $z$  and/or  $1/D$  increases.

This effect is best understood by examining the interference patterns which constitute the hologram. These circular fringes have a normalized intensity in the far field given by Ref. 1.

$$I(\rho) = 1 - \frac{d}{\rho} \sin\left(\frac{\pi\rho^2}{\lambda_1 z}\right) J_1\left(\frac{\pi\rho d}{\lambda_1 z}\right) + \text{negligible terms} \quad (2)$$

Figure 10a illustrates Eq. (2) for a constant particle diameter of  $160 \mu\text{m}$  at three distances from the film plane. The dashed lines indicate zeroes of the Bessel function,  $J_1$ . As more zeroes of the Bessel function are recorded, the sharpness of the image improves. It is usually assumed that to resolve an image, information out to at least the first zero is accurately recorded. The radius of this minimum resolution hologram,  $\rho_m$ , is given by

$$\rho_m = 1.2 \frac{\lambda_1 z}{d} \quad (3)$$

As  $z$  increases, the intensity variations decrease in amplitude, and at some radius,  $\rho_m$ , the intensity is lost in the noise of the recording, thus limiting the effective size,  $2\rho_m$ , of the hologram. To achieve good edge detail, at least three zeroes of the Bessel function are desirable (Ref. 8).

Figure 10b illustrates Eq. (2) for a fixed distance,  $z$ , for three particle radii. Again, the amplitude of the intensity variations decreases as the size,  $d$ , decreases, leading to a similar effect in limiting attainable  $\rho_m$ .

In both examples, Figs. 10a and b, it is shown that fringe frequency increases with  $\rho$ , a fact which requires film resolution to be higher for larger effective hologram sizes.

Interference fringe characteristics are commonly discussed in terms of a parameter called far-field number, which accounts for both particle size and distance. One far-field distance is defined as

$$Z \equiv d^2/\lambda_1$$

where  $\lambda_1$  is the recording wavelength. As a rule of thumb, a hologram should be made within 100 far-fields of the particle. Since this number depends upon many noise-generating factors, it can vary by an order of magnitude in either direction and must be used with caution.

#### 2.4.2 Image Motion During Recording

The effects of image motion during recording can be seen in terms of Fig. 10a. As the particle moves with respect to the recording medium, the fringes of the interference pattern are smeared, especially at the high spatial frequencies normal to the direction of travel, thus reducing the effective diameter of the recorded diffraction pattern for reconstruction. Small amounts of motion do not significantly affect the low frequencies. Motion smears the high-frequency fringes and places more restriction on the holographic recording as the particle size decreases and as the distance,  $z$ , increases. The usual criteria stated is that a particle should not move more than one-tenth of its diameter during a recording. This criteria is quite arbitrary and, in fact, if a particle moves by several diameters during a recording, the image will be reconstructed as a streak. However, the intensity and resolution will be reduced (Ref. 9).

### 2.4.3 Recording Volume

To this point, holographic quality has been discussed in terms of a single diffraction pattern. Particle parameters and volume dimensions can place severe restrictions on the quality of the reconstructed imagery. Number density, volume depth, and particle sizes combine to degrade the hologram recording. If these three parameters are too large, light passing unscattered through the volume is not sufficient as a reproducible reference beam.

The utility of holography ultimately depends upon the ability of an investigator to derive data from the reconstructed image. When a hologram of an extended volume of many particles is analyzed, any individual particle image is immersed both in optical noise and in light scattered from out-of-focus images. Since smaller particle images often have the same appearance as coherent optical noise, considerable skill is sometimes required to distinguish them.

The geometry of a typical hologram recording is shown in Fig. 11. The particle volume has a depth of  $L$ , and the nearest particle is a distance  $z'_0$  from the film plane. Assuming that the area of the Airy patterns of the total number of particles must be less than or equal to the area of the hologram to eliminate multiple scattering effects, then the equation and curves for  $N_2$  in Fig. 12 result. These are plots of number density for various object diameters. Number density  $N_1$  was obtained from Beer's law (Ref. 10). Regions within the solid lines indicate where high-quality in-line holograms can be made. In the outer regions, side-band holography or other optical methods would be appropriate.

Besides the particle parameters, density gradients in the volume can deteriorate image quality. If it is assumed that these introduce a phase change of  $\theta_r$  into the reference beam and  $\theta_o$  into the object beam, then the intensity in the recording is

$$I = |A_o|^2 + |A_r|^2 + 2A_oA_r \cos [(\phi_o - \phi_r) + (\theta_r - \theta_o)] \quad (4)$$

This general equation applies to both in-line and off-axis holography. In the later case,  $\theta_r$  is zero, since the beam is carefully routed around the test region. The hologram will then reconstruct the phase distortions on the image. However, in cases where these distortions are small, then for an in-line hologram  $\theta_r = \theta_o$ , and the reconstructed images are undistorted. Therefore, although the density gradients can affect the

reference beam of an in-line hologram as well as the object beam in certain instances, the effects will cancel, whereas in side-band holography they will not. Cases in which the in-line hologram can withstand more phase aberrations than the off-axis hologram and reconstruct accurate images still remain to be investigated.

#### **2.4.4 Film Properties**

Film characteristics have been discussed to some extent in terms of Fig. 10. In summary, it was shown that smaller particle sizes, larger particle distances from the recording, and higher resolution of the reconstructed image require higher resolution film and that system noise is a significant factor in these cases. For every holographic recording, the effective diffraction pattern diameter is limited either by the film noise, resolution, or physical size, or by a combination of these factors. This effective diameter and the distance of the object from the hologram define the recorded solid angle of light, and, therefore, the maximum resolution in the reconstructed image. Films are available that minimize the above factors, and these are especially suited for holography.

#### **2.4.5 Laser Characteristics**

Highly coherent lasers are now commonly available, and coherence is no longer a limiting factor in hologram recording, especially for the in-line case. If, however, a laser does exhibit a low spatial or temporal coherence, the ultimate effective diameter of the diffraction pattern which will be recorded is limited. A more common limiting factor occurs when a laser of one wavelength is used for the recording while a laser of a second wavelength is used for reconstruction. This introduces chromatic aberration into the reconstructed image.

#### **2.4.6 Reconstruction Geometry**

Ideally, the reconstruction wavelength and geometry should be identical to the reference beam in the formation of the hologram. Any difference in these two introduces image aberrations which are similar to those of a lens system. For this reason, it is advantageous to use collimated light for the formation and reconstruction of in-line holograms, since it is easier to duplicate in the reconstruction.

## SECTION III MULTIPLE EXPOSURE HOLOGRAPHY

### 3.1 BASIC THEORY

Multiple exposure holography provides three types of object data, depending on how the holograms are recorded and on their specific application. In one case, two holograms of a large object undergoing a physical change are superimposed on a single recording. The two stored waves reconstruct simultaneously and interfere, indicating small amounts of change between the two exposures. This is the basis for holographic interferometry. In a separate context, multiple-exposure holography refers to the storage of more than one hologram upon a recording medium with different reference beams for each recording. Individual wavefronts can thus be constructed independently. In the present context, recording the time history of a moving object is the concern. The reconstruction, therefore, will include multiple images of the object where the difference in the images (and not the actual interference of the two reconstructed waves) is of interest. For example, the time interval between two exposures and the separation of an image pair yields the average velocity of the particle.

The basic theory and equations describing this process are included in Refs. 2 and 11. Based on a summary of the results, the following conclusions are reached:

1. The overall photographic density for an optimum multiple-exposure recording is greater than that for a single-exposure recording.
2. Such a recording process is rarely linear, and in fact the best results are obtained by recording in a nonlinear recording region of the film.
3. The quality of a hologram decreases with the number of recordings because of optical and photographic noise.
4. The largest exposure produces the brightest reconstruction. This fact is useful for indicating the direction of motion.
5. Dynamic range limitations of the film ultimately limit the total number of exposures which can be superimposed on the film.

6. Coherence between separate recordings is unimportant in this type of recording.

Figure 13 illustrates the data that can be obtained from a double-exposure hologram. The double-pulsing ruby laser described in Section 3.2.2 was used in a simple in-line holographic system to form a recording of a flow field of magnesium oxide particles. In the center of the figure is an enlarged portion of the hologram. Pairs of diffraction patterns are seen throughout the figure. Each pattern of the pair indicates the location of a single particle at the time the holograms were made. Photographs of some of the particle reconstructions are also shown in Fig. 13. The higher velocity, smaller particles, which are rapidly accelerated, are more widely spaced than the larger particles. Particle rotation is also observed. Particles on the left side are seen to have lower velocities than those on the right side. Sizes range from 10 to 200  $\mu\text{m}$  in diameter and vary widely in shape.

## 3.2 MULTIPLE-PULSED LASERS

To record a multiple-exposure hologram requires short exposure times and an accurate, controllable separation between exposures. For slowly changing fields this can be accomplished with a continuous-wave laser and a mechanical shutter. However, application to the high velocities in dust erosion facilities requires extremely short light pulse duration times and small pulse separations. These conditions can be achieved by Q-switching a laser.

Lasers which may fulfill the necessary requirements include YAG lasers in a frequency-doubled mode. At this time, however, only ruby lasers have achieved successful results at AEDC.

### 3.2.1 Q-Switching Techniques

Many techniques are available for Q-switching a laser. These fall roughly into the categories of mechanical, chemical, and electro-optical. Mechanical Q-switches depend upon the precision alignment required of the two end reflectors of a ruby laser. A reflector is mounted on a vibrator or rotating drum and is moved into alignment at the proper time during the laser flash lamp sequence. Short light pulse widths result from the rapid motion of the mirrors.

Another type of electro-mechanical Q-switch places an end reflector in the cavity for a short period of time. Such a scheme is illustrated in Fig. 14. In the spoiled mode, the prism separation is large enough so that total internal reflection in the left prism occurs, and this allows light to pass along the dotted line out of the cavity. When the distance S is less than a few wavelengths, the internal reflection is reduced, and lasing occurs. The time required to displace the upper prism through a few wavelengths can be made very small by driving it with a piezoelectric crystal. This relatively new technique offers an extremely promising and efficient way of Q-switching. It has been used in other laboratories, successfully providing Q-switched pulses as close as 1  $\mu$ sec in separation. Because of its high efficiency, the energy in the pulses can be easily adjusted. Although mechanical Q-switches are not employed at AEDC at this time, it is expected that they will be tested in future work.

A number of chemicals possess absorption characteristics which allow them to be used as Q-switches. The chemical (dye in solution) is placed in a transparent container within the cavity. Because it is highly absorbent at the laser wave length, it initially spoils the cavity efficiency and inhibits lasing. However, when the intensity of the light reaches a certain level, the absorbing molecules are depleted; saturation, or bleaching, occurs, and the chemical becomes momentarily transparent at the laser wavelength. Such chemicals include cryptocyanine dye in alcohol or acetone solution and chlorophyll-D (Ref. 12) in mineral oil solution. These Q-switches are somewhat erratic and troublesome to use because the chemicals are neither stable nor completely reproducible, and they are sensitive to both temperature and light. A number of techniques, however, have been developed to eliminate some of the disadvantages.

Chemical Q-switching is attractive because of its inherent efficiency, simplicity, and high coherence. Either of the chemical Q-switches can be used for multiple pulsing when the laser flash lamp energy is large enough and the solution is properly mixed. With extensive care, one can produce double pulses with separations ranging from 1  $\mu$ sec up to about 200  $\mu$ sec. However, it is somewhat difficult to repeat or to predict exactly how the Q-switch will function. Q-switches were initially used at AEDC, but because of their sporadic performance they have since been replaced by other more reliable electro-optical devices.



Pockell's cells and Kerr cells are electro-optical Q-switches. Their operation is based on the fact that, by an applied voltage, the light polarization can be changed as it passes through these crystals. The cavity efficiency, or Q, is made highly dependent upon polarization with a so-called Brewster stack, which passes nearly 100 percent of one polarization component within the cavity while stopping the other. These Q-switches employ more optics and electronics than any of the other types and are, therefore, more expensive and optically less efficient. However, they have one distinct advantage over all other types; since the time of Q-switching is electronically controlled, the laser light pulse can be initiated within a few nanoseconds. Because of its poor efficiency, multiple Q-switching is accompanied by a sacrifice of laser power. To maintain output power levels near maximum, the two light pulses are required to have a separation exceeding approximately 50  $\mu$ sec. Commercial units operating at faster pulse repetition rates and lower laser power are available at pulse separations down to about 1  $\mu$ sec, but at low power levels.

Finally, a relatively new technique termed "cavity dumping" is applicable, especially to continuous-wave (CW) lasers. Optical energy built up in the cavity of a CW laser which has high reflecting end mirrors can be dumped by electro-optically removing an end reflector from the laser. This provides increased laser power and very short pulses. The cavity can be "dumped" at rates up to about 100 MHz. These lasers provide great potential for high-speed motion-picture holography. Figure 14 illustrates the cavity-dumping technique.

### 3.2.2. AEDC Double-Barreled Ruby Laser

Based upon earlier work at AEDC and following suggestions made by engineers of the Union Carbide Korad Division, a double-barreled Pockell's cell Q-switched laser was designed and constructed at AEDC. Figure 15 illustrates the general layout of the AEDC double-barreled ruby laser and the block diagram of the controlling electronics. The cavity is divided into two sections by a pair of apertures, each 2mm in diam. The two sections, or barrels, of the laser form two independent laser cavities with the one ruby rod. Each is Q-switched separately, with a time delay between the two. The two laser light pulses are separated by times as short as 0.4  $\mu$ sec and up to 1 msec. Shorter delays are conceivable. The only limitation to the repeatability of the separation is jitter in the firing circuits of the Pockell's cells electronics. The largest separation is limited by the duration of the flash lamp.

It is important to note that, since two independent cavities exist, the frequency of the two light pulses is slightly different. This system could not be used without special adjustments to make multiple exposure holographic interferograms, since the waves in the two laser pulses are not coherent with each other. As previously stated, this is unimportant for the multiple-exposure holograms under consideration here. The two output beams of the laser are parallel and are separated in space. They are recombined with a parallel plate beam combiner in the scheme shown in Fig. 16. Fifty percent of the laser light is lost. Because of the extremely accurate recombination of the two beams, the optical system for the holocamera is the same as that for a single-beam laser, even down to the spatial filter and beam-expanding lens.

## SECTION IV AUXILIARY INSTRUMENTATION

### 4.1 RECONSTRUCTION SYSTEM

The dust particle volume is reconstructed by illuminating the hologram with laser light. A typical reconstruction setup is shown in Fig. 17. Collimated light from a helium-neon (He-Ne) laser illuminates the hologram. A lens,  $L_1$ , magnifies the reconstructed images (real or virtual), which are then focused onto the face of a closed-circuit television (TV) camera vidicon tube and observed on the monitor screen. A wire grid is imaged on the vidicon tube by lens  $L_1$  for calibration purposes. The TV camera and  $L_1$  remain fixed after the desired magnification is set. The reconstructed volume is scanned by moving the hologram and, consequently, the reconstructed images in three orthogonal directions.

Reconstructed images can initially be scanned under low magnification to provide a quick examination of the volume. Portions can then be enlarged by increasing the distance from  $L_1$  to the camera and maintaining focus with the hologram. Noise from irregularities on glass surfaces in the reconstruction system usually limits useful lens magnification to about six. The television system electronically magnifies the images approximately 35 times, giving an overall maximum magnification of 210X.

Measurements are commonly made at the monitor screen, either with a calibrated scale or by moving the image across a fixed line with

a calibrated traverse. For velocity data, the separation between the image pairs is also measured this way. The reconstruction distance is read directly from scales on the optical bench.

Although a closed-circuit TV system greatly facilitates data reduction from holograms, it is, of course, not absolutely necessary. Direct recording of the reconstructed image can be provided by photography. Moreover, the spatial image can be viewed directly with a microscope or an eyepiece, although the latter not only requires extra safety precautions, but is extremely tedious in data reduction. Direct viewing is further complicated by the shortcomings of the eye in viewing coherent light and by its lack of sensitivity to red light.

## 4.2 COMPUTERIZED HOLOGRAPHIC DATA ACQUISITION SYSTEM

A single in-line hologram of a particle field can reconstruct thousands of images. Analysis of each for size, velocity, and position becomes a tedious, costly, and time-consuming process.

To augment data acquisition, a computerized image analysis instrument (trademark  $\pi$ MC) (Ref. 13) has been incorporated into the AEDC reconstruction system. It measures the area or length of light or dark objects on the TV monitor, thus reducing measurement time and operator fatigue. This instrument in the reconstruction system is shown pictorially and in block diagram in Fig. 18a.

The video signals of the images focused on the vidicon are analyzed by the measurement system. A particle image is "sensed" according to a threshold trigger control, and the images are tagged and outlined on the monitor. This allows the operator to observe the images which are being electronically analyzed. Pressing a remote switch displays the measurement and count at the top of the monitor screen and initiates the printout on paper or magnetic tape. The system is capable of measuring the height, width, longest dimension, area, and the total number of images on the monitor.

The monitor photograph in Fig. 18a illustrates the display for an average area measurement of the reconstructed images. The outline of the measured areas is intensified on the monitor and tagged at the lower left. For length measurements, only the right of the image is outlined.

Two different modes of operation can be employed; one measurement includes all the images on the monitor, and the other measures individual images selected by the operator. The former is most useful when the reconstruction is relatively noise free. It provides the following measurement capabilities: (1) average image width and area, (2) total number of images, (3) total width and area of all images, and (4) number of images exceeding a selectable width or area. Number (4) provides a size distribution capability. Since the image analyzer triggers on a selected voltage level (or image intensity), high optical intensities of out-of-focus images on the monitor are not distinguished from in-focus images and are analyzed in addition to in-focus images. The same problem applies to high optical noise intensities. This often requires an operator to decide which are in focus and, therefore, leads to the second mode of operation.

In this mode of analysis, only those images which are designated by a light pen (used by the operator) are analyzed. Figure 18b shows the light pen and plug-in module, and Fig. 18c illustrates its use for individual measurements. With the pen close to the monitor screen, a crescent-shaped "pointer" is generated. When the bottom of the crescent touches the top of the particle image, a white line surrounds the image to show it is being sensed. Pushing the tip of the pen against the screen activates a microswitch, causing the measurement to be displayed.

In the light-pen mode, the operator distinguishes between in-focus images and noise on the TV monitor. Although not a present capability, the in-focus condition could be determined automatically by electronically monitoring the image slope and initiating the measurement when it reaches a maximum along a z-dimension scan (Ref. 14).

### 4.3 LIGHT PULSE COUNTER AND TIME SEPARATION ELECTRONICS

An important parameter in the velocity calculation is the separation between the two light pulses. Jitter in the Pockell's cell and time-delay electronics and changes in the parameters in the timing circuit caused by temperature effects can change the separation of the laser firings. Consequently, an instrument which can detect and display the interval between the two pulses is necessary. The system developed at AEDC to accomplish this is shown in Figs. 19 (schematic) and 20.

Light is detected by a photo-diode, and the signal is amplified and shaped. At point A, the pulses are counted and their number displayed. A count of three signifies that three or more pulses were detected. This feature of the device is particularly necessary if a dye cell is used. The dye can become saturated two or more times during the flash lamp cycle when enough energy is expended into the ruby rod (see Section 3.2), causing multiple laser pulses.

The two pulses from the wave-shaping circuit also open and close a gate through which passes a train of pulses from a stable, high-frequency (100-MHz) local oscillator. The pulse train is counted and displayed by light-emitting diode arrays as the time interval of the light pulses. Once the gate has opened and closed, it is inhibited until a manual reset button is depressed. This also sets the readouts to zero for the next measurement.

The accuracy of this device depends on the clock frequency, the slopes of the signals that trigger the wave-shaping circuit, and the opening and closing of the gate relative to the phase of the clock pulse. In the latter case, this is  $\pm 1$  clock pulse, corresponding to an inaccuracy of  $\pm 10$  nsec.

## SECTION V IN-LINE HOLOCAMERA SYSTEMS

### 5.1 BASIC SYSTEM

Figure 21 illustrates the holocamera system which has been used extensively at AEDC. Individual components of the system are labeled. A few of the more important elements of the system will be discussed in detail. The CW He-Ne laser is used for alignment of the optics. Through an autocollimating procedure, the path of this beam is made coincident with the ruby laser beam. Autocollimation is accomplished by centering the He-Ne light reflected from the front ruby laser mirror back into the He-Ne laser.

An important feature of the camera system is the beam expander-spatial filter. At present, this system employs a 20X microscope objective which focuses light through a pinhole. A neutral density filter reduces the light level to a value that is safe for the optics. Both the front element of the microscope objective and the pinhole are easily

destroyed by the high-intensity light. To remedy this somewhat, the front element of the microscope objective has been replaced with an uncoated, simple lens, since the weakest portion of the lens is the optical coating and cement.

The spatial-filtering pinhole must also be carefully selected to avoid destruction. If this pinhole is originally chosen to be of a diameter which is usually employed with CW lasers (on the order of 10 to 20  $\mu\text{m}$ ), the laser pulse will enlarge this hole to an unacceptable diameter, and such a pinhole would be useful for only a single shot. Furthermore, alignment would be extremely difficult. It has been found that if the pinhole is of a larger diameter (100  $\mu\text{m}$ ), it will not be destroyed by the laser pulse and, moreover, alignment will be considerably simplified. Complete spatial filtering is not attained, nor is it necessary in most cases. Figure 22 illustrates the effectiveness of various diameter spatial filters for a 20X microscope objective. A 30- $\mu\text{m}$  diam pinhole is an excellent filter. Even one of 100- $\mu\text{m}$ -diam offers a considerable improvement over the unfiltered condition, which contains not only a considerable amount of coherent noise, but also multiple reflections between various lens components. A dirty lens system was purposely chosen, and to augment the illustration, a 10- $\mu\text{m}$  wire was stretched behind the lens.

The remaining portions of the holocamera correspond to the design discussed in Section 2.3.

This configuration has been used in many tests at AEDC and is basically the same one that was employed at the Northrup and Boeing dust erosion facilities mentioned earlier. In those installations, however, the Q-switch was a dye cell.

## 5.2 AEDC DUST EROSION FACILITY HOLOCAMERA

A permanent holocamera is installed in the AEDC PWT Dust Erosion Facility. This system, as it is mounted near the test chamber, is illustrated in Fig. 23. It was designed so that it could be operated in either the in-line or off-axis mode. At the present time, the in-line mode of operation has provided the necessary data.

Systems prior to this one were operated by manually charging and firing the laser and exchanging the film. These procedures are now automated and integrated into the test sequence. A signal from the

control room initiates the holography data cycle which charges the laser, opens shutters, fires the laser, advances the film, and restarts the cycle. This allows a maximum number of holograms to be made during the test. The cycle may also be stopped or held (after the laser is charged) from the control room. The holograms are recorded on 70-mm film instead of on glass plates.

Because of the erosive nature of the testing, windows rapidly become severely degraded. Windows used in laser systems must be of high homogeneity and nearly bubble- and scratch-free. During long test runs or after a number of short runs, the windows become badly pitted. In fact, with certain types of models which reflect dust directly toward the windows, the window quality is deteriorated beyond use during a single run. Regrinding of the windows is a time-consuming and expensive process; therefore, a window protection system was required. The system shown in Fig. 24 was devised so that only a small portion of each window surface is exposed. Unexposed portions can be easily rotated into position. Quick-opening electric shutters shield the exposed window area from impinging dust except during the hologram recording.

## SECTION VI TYPICAL EXPERIMENTAL RESULTS

The holocamera systems described have produced a vast amount of data. In this section, typical holograms are illustrated to show the types of data which have been acquired.

### 6.1 DATA TAKEN AT THE BOEING AND NORTHROP FACILITIES

Holograms taken during the Boeing and Northrop tests are shown in Fig. 25. A volume approximately 10 cm in diam by 30 cm in length (with the major length normal to the wind tunnel centerline) was reconstructed and analyzed for particle size and number density in both tests. This volume was immediately in front of a particle catcher (seen at the left of the figure) which was being used for calibration. In fact, the purposes of the holography studies were to provide an alternate calibration measurement of dust density and observe the spatial distribution of dust within the test cell. A particularly interesting observation can be made of particles rebounding from the catcher, passing through the bow shock, and entering into the free stream (Fig. 25). These

rebouncing particles were observed to significantly alter the shock front. Upon entering the free stream, each was characterized by an unusually strong shock. In addition to particle reconstructions, the shock waves were also reconstructed as sharp lines. The unusual strength of the shock associated with these particles was connected to their penetration of the strong bow shock. Other effects which were observed on the hologram print, as well as in the reconstruction, included instabilities in the aerodynamic flow, turbulence generated by rebouncing particles, and instabilities of the catcher. In some instances, severe distortions of the bow shock could not be associated with any particular particle. These distortions were considered to be caused by pressure pulses expelled by the catcher.

During each of 33 runs, two holographic recordings were made. Data were taken from a total of 60 holograms. Part of the test was concerned with comparing particle density at two separate times during the tunnel operation. The holographic recording, as opposed to other instrumentation techniques, is practically instantaneous, and, therefore, provides particle information for one instant in time (during the pulse width of the laser). The two recordings made during each test indicated that in some instances, large variations existed in the test cell during the two hologram exposures. However, in other instances, the particle number densities at the two separate times were reasonably close. It was established that average measurements for one set of tunnel conditions would require more than two holograms. An unexpected number of smaller particles was observed in the reconstructions. The holocamera resolution was determined to be at least  $20\ \mu\text{m}$  or better.

## 6.2 AEDC TEST DATA

Figure 26 is a double-exposure holographic recording made in the PWT Dust Erosion Facility during standard model testing. Double diffraction patterns can be seen throughout the recording. The separation between the two exposures for this case was  $0.45\ \mu\text{sec}$ . Figure 27 illustrates the image pairs reconstructed within a small region of the hologram of Fig. 26. Typically, from 200 to 300 image pairs are reconstructed in a volume approximately 8 cm in diameter and 30 cm in depth. Figure 28 illustrates the correlation between size and velocity from measurements of the reconstructed images. The mean velocity is symmetrical about the test section centerline and decreases with increased particle size.



These data correlate well with data taken with laser Doppler velocity measurements and fiber-optic particle size measurements.

## SECTION VII FUTURE PLANS AND REQUIREMENTS

### 7.1 FAST RECORDING RATES (CINEHOLOGRAPHY)

The laser system discussed in Section 3.2.2 allowed two hologram exposures to be made with time separations ranging from approximately 0.5 to 1000  $\mu$ sec. This separation is quite satisfactory; however, in many dynamic situations a sequence of such recordings is needed with time spacing ranging upward from 1 msec to give a time history of the event. Many additional exposures could be made during the laser flashlamp firing (Section III), or the flashlamp could be recharged. Repetition rate is presently limited by the charging time of the power supply, which varies from 5 to 15 sec, depending upon the time constant of the charging circuit. Certain commercially available power supplies reduce this time to less than 1 sec.

The ultimate flashlamp recycling rate achievable is limited, not by the power supply or flashlamp, but by the requirement to maintain the ruby rod at an acceptable temperature. This introduces new factors into the design of systems with increased recording rate. The rod must be small (large surface-to-volume ratio), well cooled, and operated at low power. Continuous-wave operation is now possible, but only at power levels considerably below most recording requirements. Even when this condition is met, the laser coherence is reduced significantly by temperature gradients in the crystal.

To compensate for these effects, compromises can be made in film resolution, hologram size, and signal-to-noise ratio in the reconstructed image. The optimum compromises should be examined for practical applications. The method of cavity dumping described previously should be examined to determine its capability for increasing hologram recording rates.

Two types of recording procedures are envisioned, (1) multiple recording on a single frame and (2) multiple-frame recording. The applicability of these methods to testing should be studied.

## 7.2 AUTOMATED DATA REDUCTION

Particle data are reduced from the hologram in several ways. The images on a TV monitor can be measured with a calibrated scale, or the hologram can be mounted on a micrometer traverse and the image moved across a fixed point on the monitor screen. The reconstruction distance is usually read from the optical bench. Coordinates in the plane of the hologram can also be taken from calibrated scales with indicators mounted on the hologram traverse. Up to now, all of these data have been recorded by hand, a process resulting in much needless data handling.

A motorized traverse system with a digital position readout in conjunction with the automatic image analyzer (discussed in Section 4.2) would greatly reduce the data reduction time. A system currently being designed is illustrated in block diagram in Fig. 29, and the control console and associated optics are sketched in Fig. 30. The operator controls the hologram position with joy sticks. Pulses from optical shaft encoders are counted for a readout of the x-y traverse position. Motion along the optical axis (z-dimension) produces a corresponding voltage change which is displayed on a digital voltmeter. Digital-to-analog converters move a pointer on an x-y recorder to indicate the location on a hologram print that is being observed on the TV monitor. The print aids the operator in locating gross areas of interest on the hologram for detailed analysis. Once an image has been measured, the position and size data are transferred to paper and/or magnetic tape for storage and computer analysis.

For data where the x-y spatial coordinates of the particles are unnecessary, the width, height, and separation (for velocity data) of the images may be measured by resetting the x-y readouts to zero at the edge of the image and making the appropriate traverse.

In applications where low number densities occur or where the reconstructed volume is scanned first before data are taken, the readout system can be set on automatic scan. In this mode of operation, x and y will be incremented a fixed amount after each continuous scan through z. The operator can then stop the scan whenever he observes an image which he wishes to measure. In all cases, the limits of traverse are preset according to the reconstructed volume limits. The automatic scan mode can also conceivably be part of an entirely automatic hologram data-reduction system in which a computer detects the in-focus image condition and initiates its measurement and the data recording.

## SECTION VIII CONCLUSIONS

The design and application of holographic systems in dust erosion facilities and other related facilities have been discussed, and the following conclusions have been reached:

1. In-line holography provides an extremely valuable and versatile technique for measuring dust particle size, number density, velocity, and distribution and the distributions of these parameters in space and time.
2. Such systems are rugged enough for test cell operation.
3. A modified conventional ruby laser in the holography system provides velocity data ranging up to at least 3000 m/sec.
4. The holocamera system resolves particles as small as 10  $\mu\text{m}$ .

## REFERENCES

1. Collier, R. J., Burckhardt, C. B., and Lin, L. H. Optical Holography. Academic Press, New York, 1971.
2. Trolinger, J. D. and O'Hare, J. E. "Aerodynamic Holography." AEDC-TR-40-44 (AD709764), August 1970.
3. Champagne, E. B. "Nonparaxial Imaging, Magnification, and Aberration Properties in Holography." Opt Soc Am J, 57, January 1967, pp. 51-55.
4. Belz, R. A. and Dougherty, N. S. "In-Line Holography of Reacting Liquid Sprays." Proceedings of the Symposium on Engineering Methods of Holography. Sponsored by ARPA, conducted by TRW Systems. Los Angeles, Calif., February 1972.
5. Trolinger, J. D., Belz, R. A., and O'Hare, J. E. "Holography of Nozzles, Jets, and Spraying Systems." Proceedings of the Air-Breathing Propulsion Conference. U. S. Naval Post-Graduate School, Monterey, California, November 1972.

6. Farmer, W. M., Burgess, K. S., and Trolinger, J. D. "Holo-camera for Examination of Water Droplets in a Large High Altitude Test Cell." AEDC-TR-70-181 (AD715916), December 1970.
7. Belz, R. A., and Shofner, F. M. "Characteristics and Measurements of an Aperature-Limited In-Line Hologram Image." Applied Optics, 11, No. 10 (October 1972), p. 2215.
8. Robinson, D. M. "A Calculation of Edge Smear in Far-Field Holography Using a Short-Cut Edge Trace Technique." Applied Optics, 9, No. 2 (February 1970), pp. 496-97.
9. Trolinger, J. D., Belz, R. A., and Farmer, W. M. "Applications of Holography in Environmental Science." J Environmental Sci, 12, No. 5 (October 1969), pp. 10-13.
10. Belz, R. A. "An Analysis of the Techniques for Measuring Particle Size and Distribution from Fraunhofer Diffraction Patterns." Masters Thesis, The University of Tennessee, June 1968.
11. Trolinger, J. D., Farmer, W. M., and Belz, R. A. "Holography Techniques for the Study of Dynamic Particle Fields." Applied Optics, 3, No. 5 (May 1969), p. 957.
12. Wuerker, R. F. "Applications of Pulsed Laser Holography" in Laser Technology in Aerodynamic Measurements, AGARD-LS-49, p. 8-1 (1971).
13.  $\pi$ MC Particle Measurement Computer System. Millipore Corporation, Bedford, Mass.
14. Belz, R. A. "An Investigation of the Real Image Reconstructed by an In-Line Fraunhofer Hologram, Aperature-Limited by Film Effects." Ph. D. Dissertation, The University of Tennessee, August 1971.

**APPENDIX  
ILLUSTRATIONS**

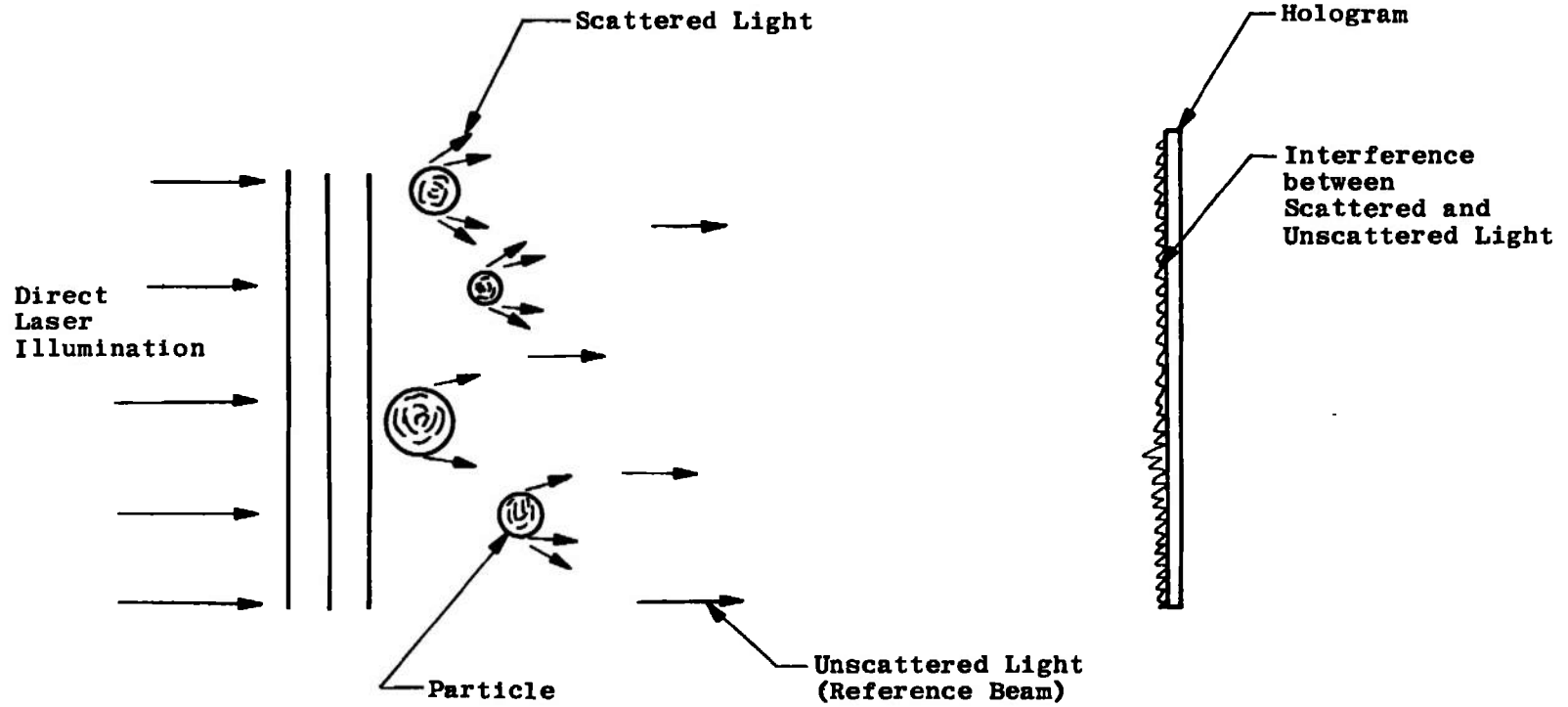


Fig. 1 In-Line Hologram of a Particle Field

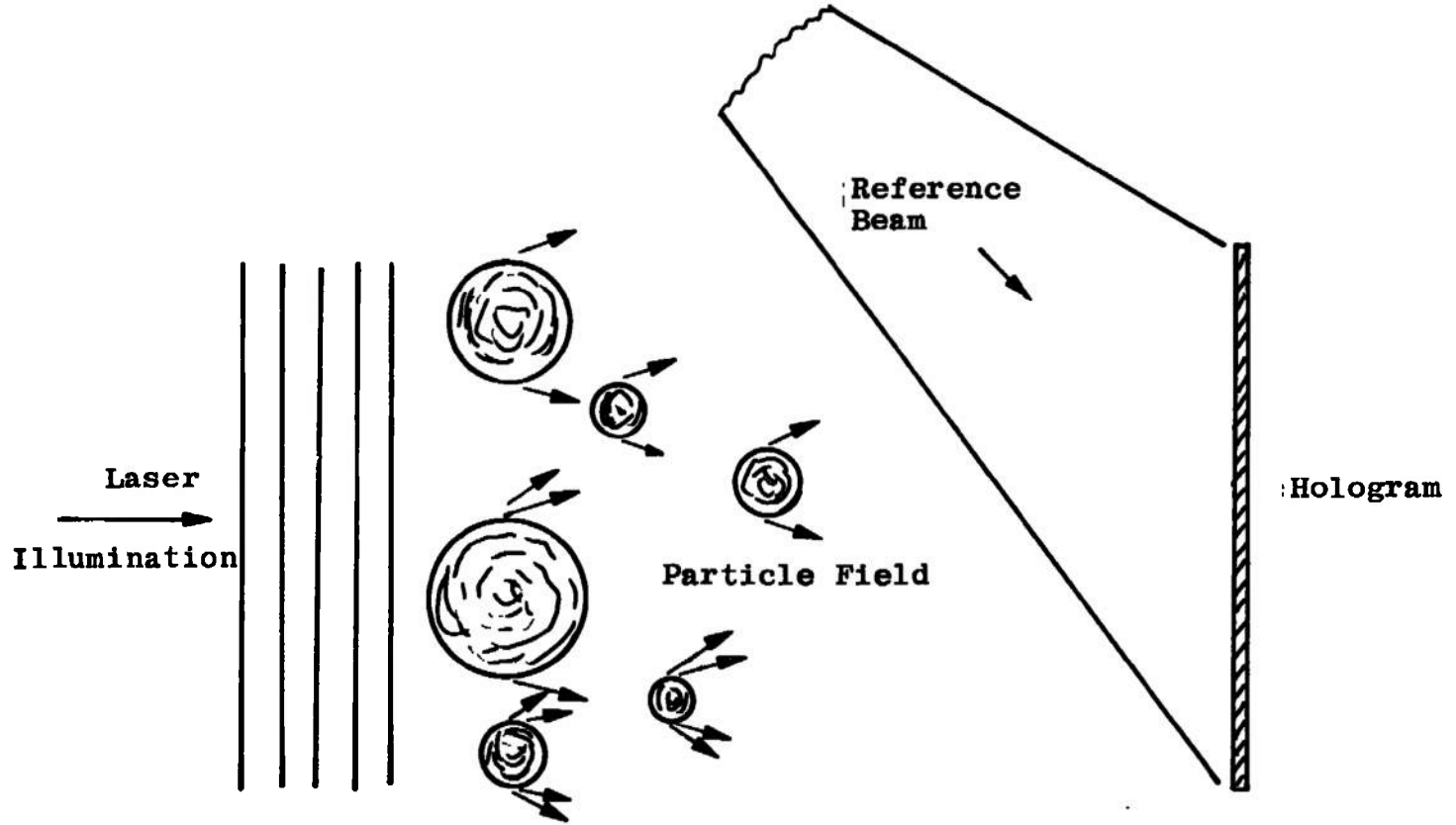


Fig. 2 Off-Axis Hologram of a Particle Field

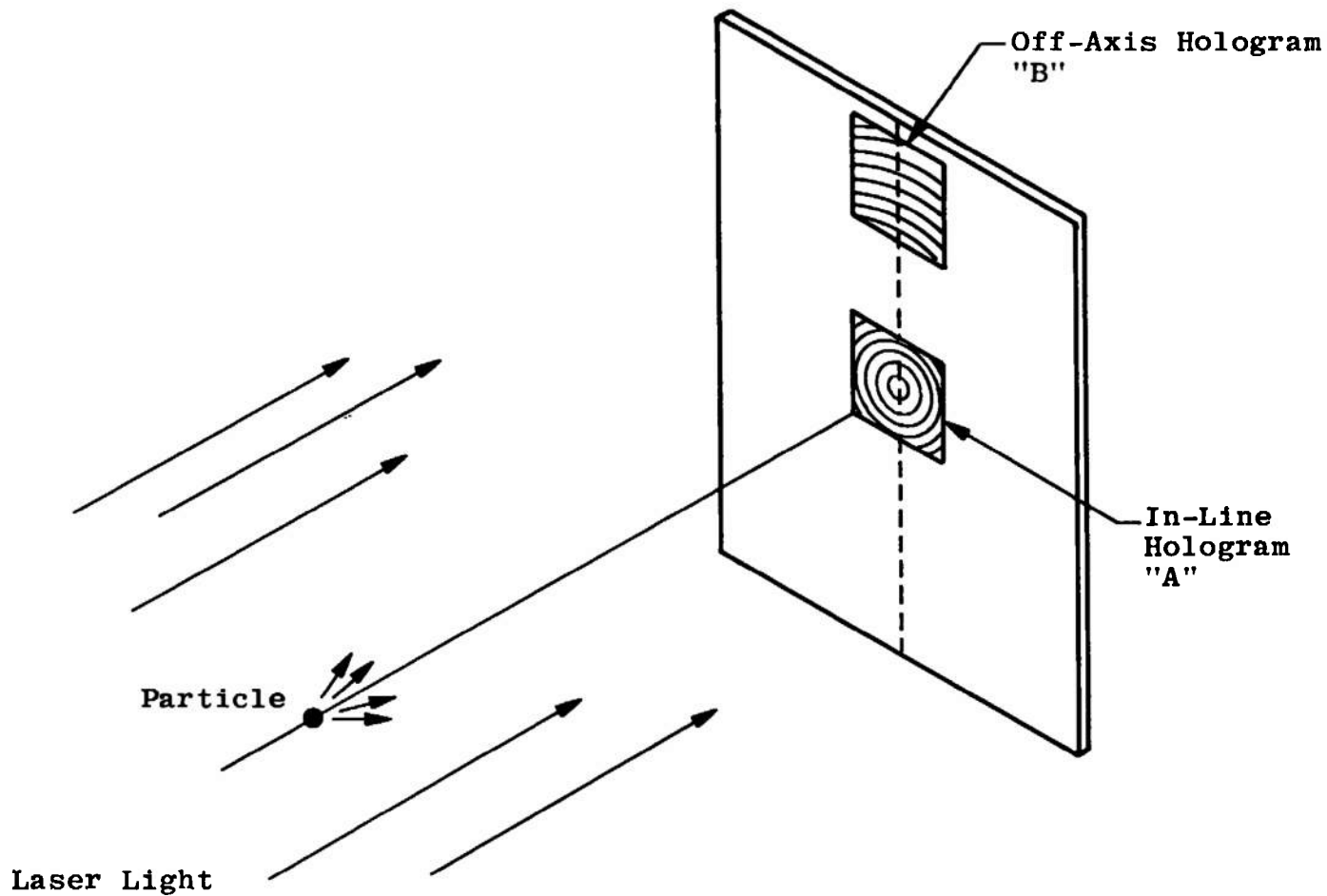


Fig. 3 In-Line and Off-Axis Hologram of a Point Object



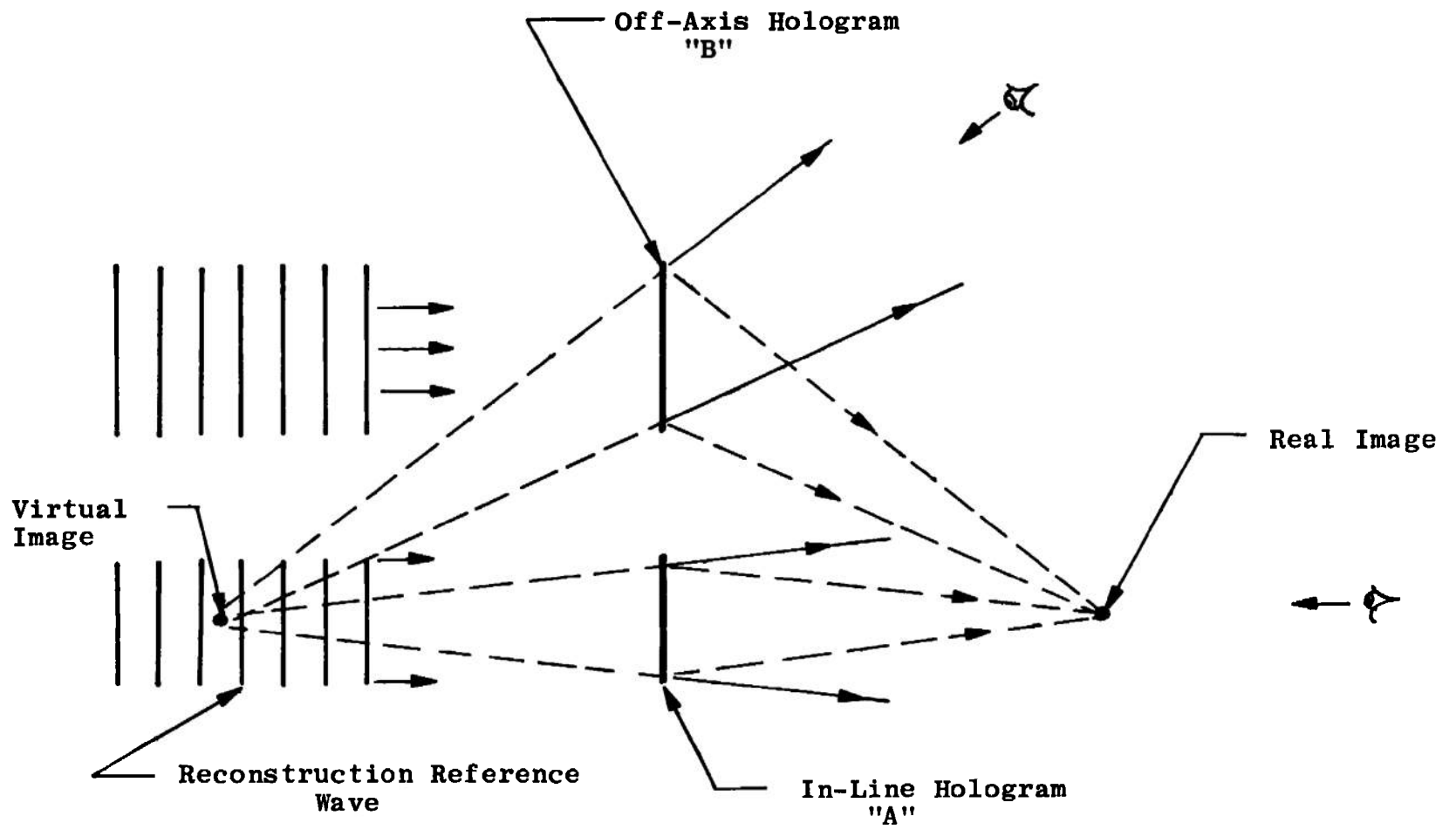
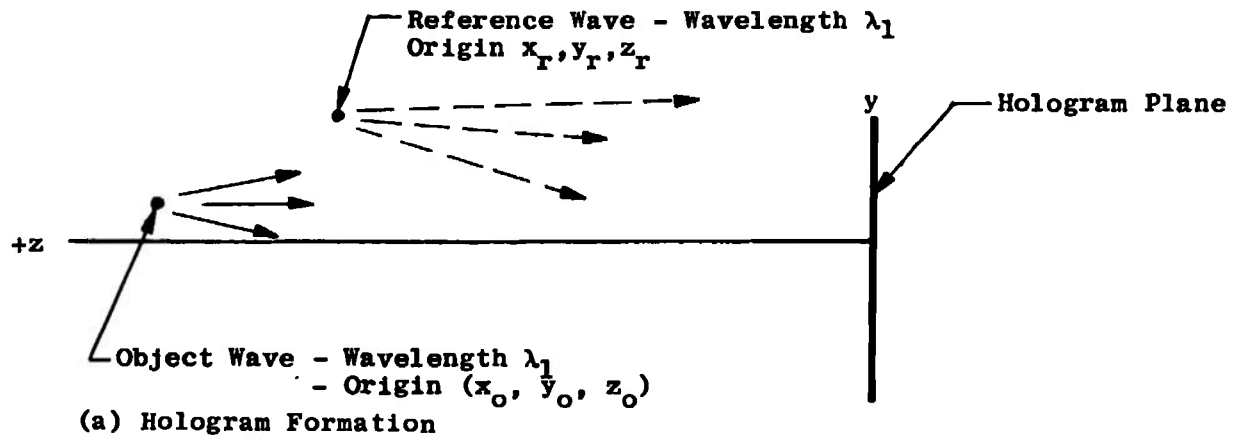
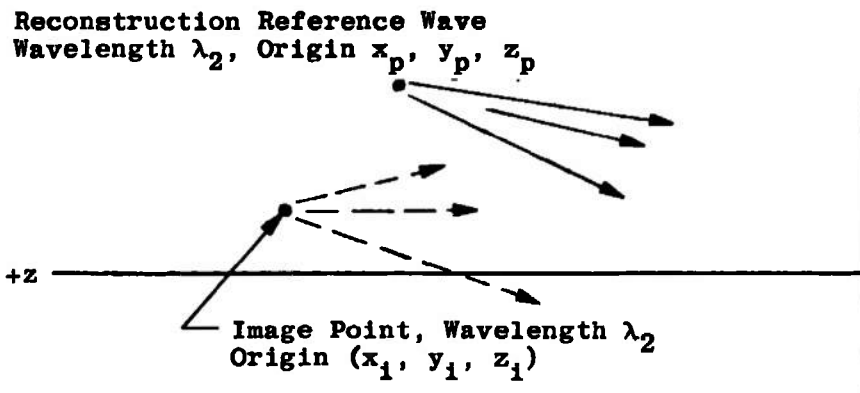


Fig. 4 Forming the Image with the Hologram of Fig. 3



a. Hologram Formation



b. Reconstruction

Fig. 5 Geometry for Equation 1

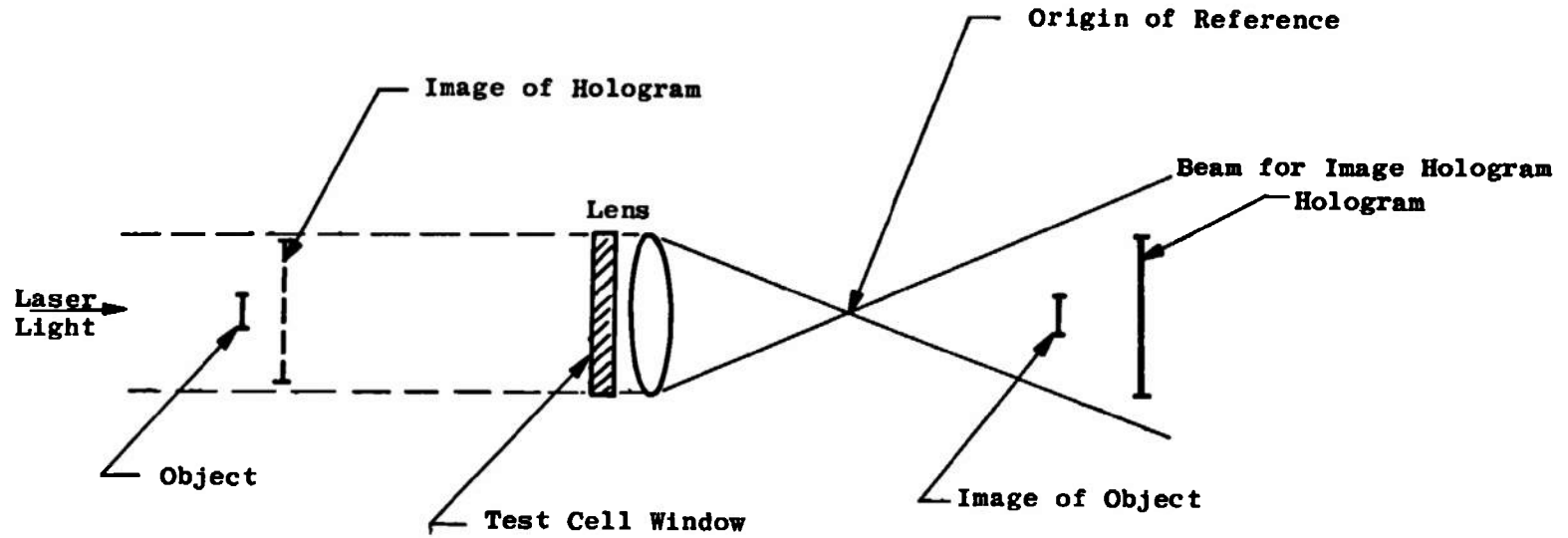
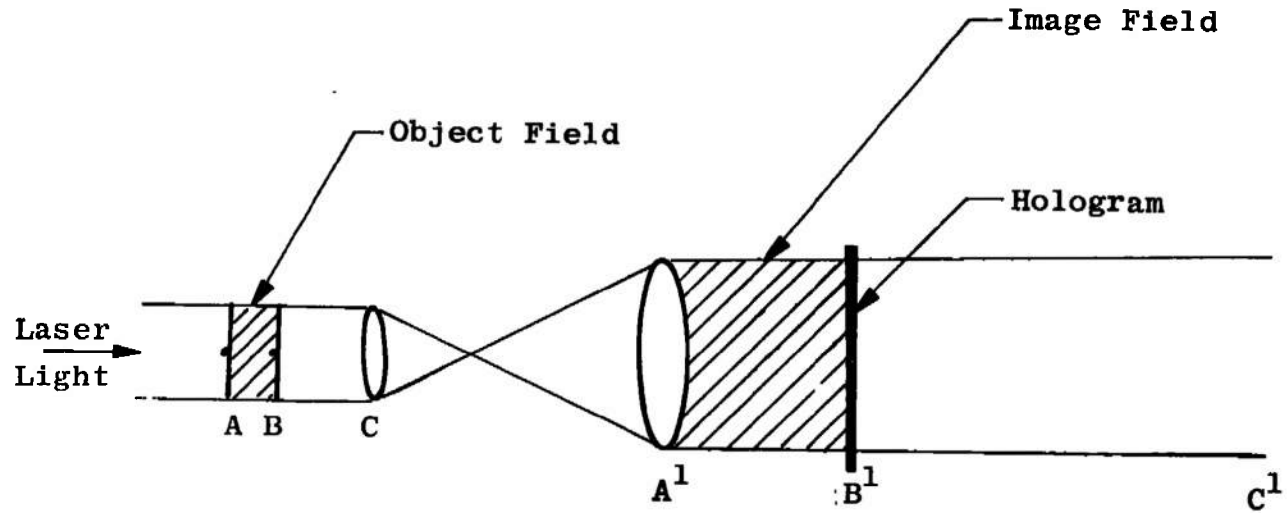
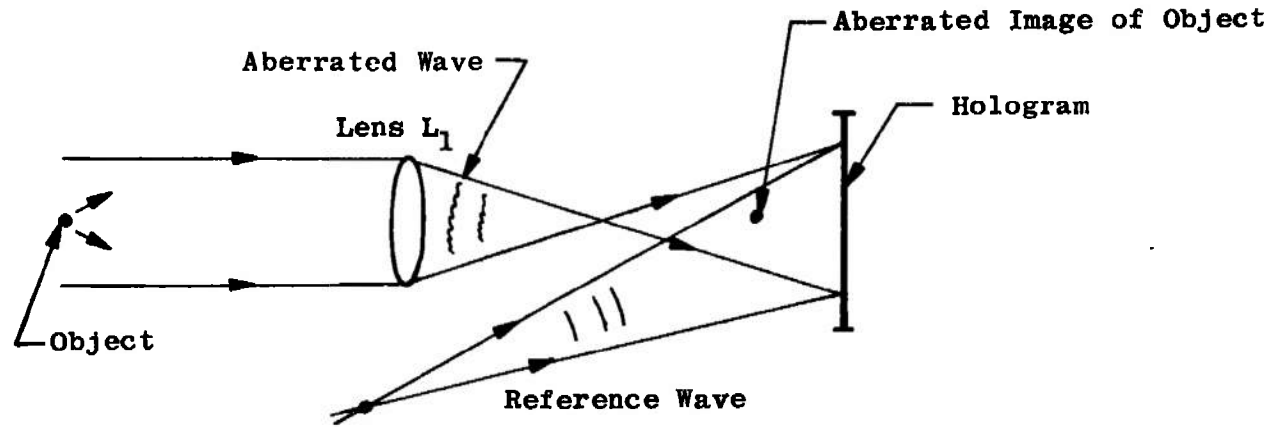


Fig. 6 Equivalent Hologram Position in Image Holography

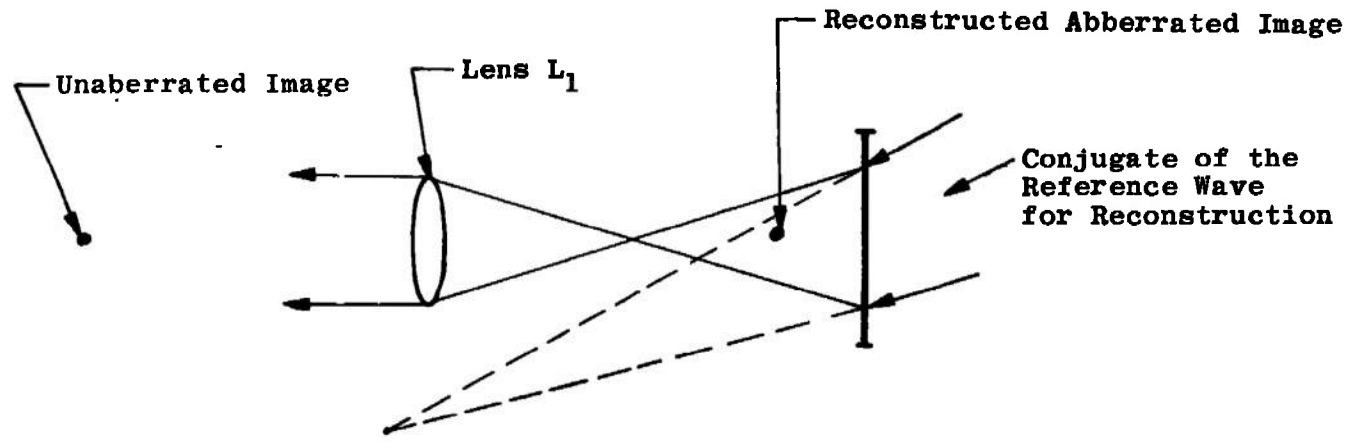


NOTE: Primed letters indicate image planes of corresponding letters.

Fig. 7 Collimator Image Transfer System



a. Producing the Hologram



b. Reconstruction and Aberration Removal  
Fig. 8 Image Holography with Aberration Cancellation

NOTE: Primed letters indicate image planes of corresponding letters.

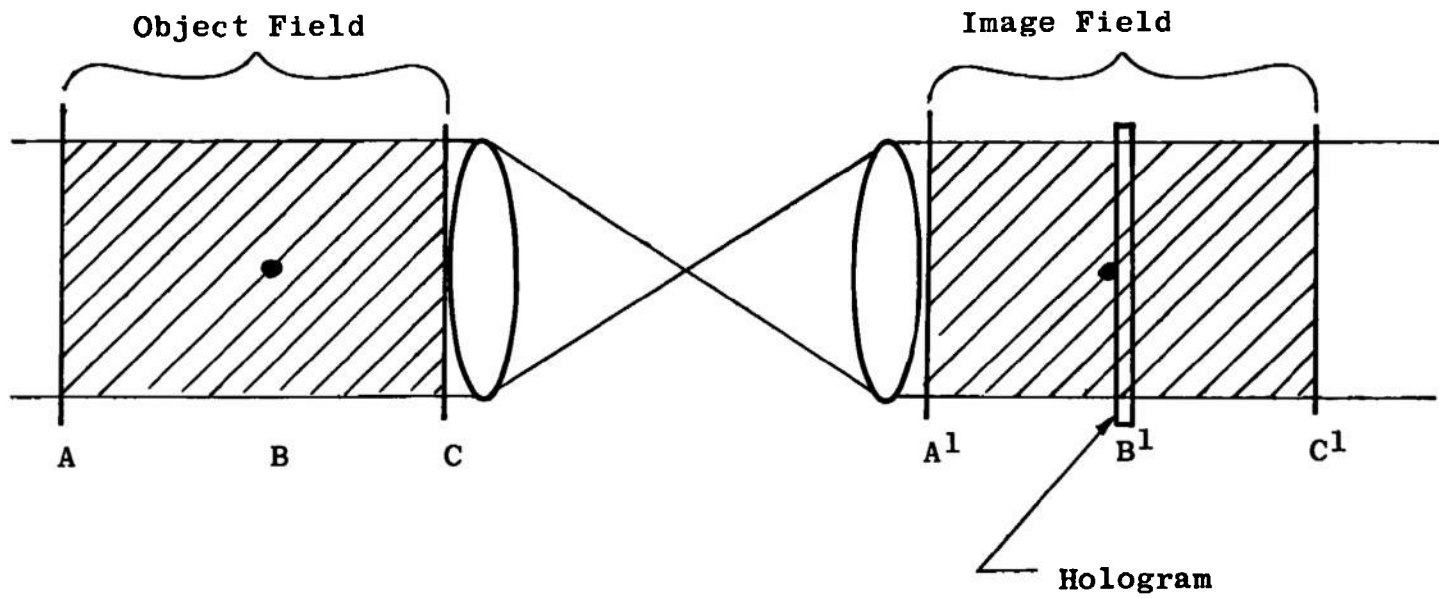
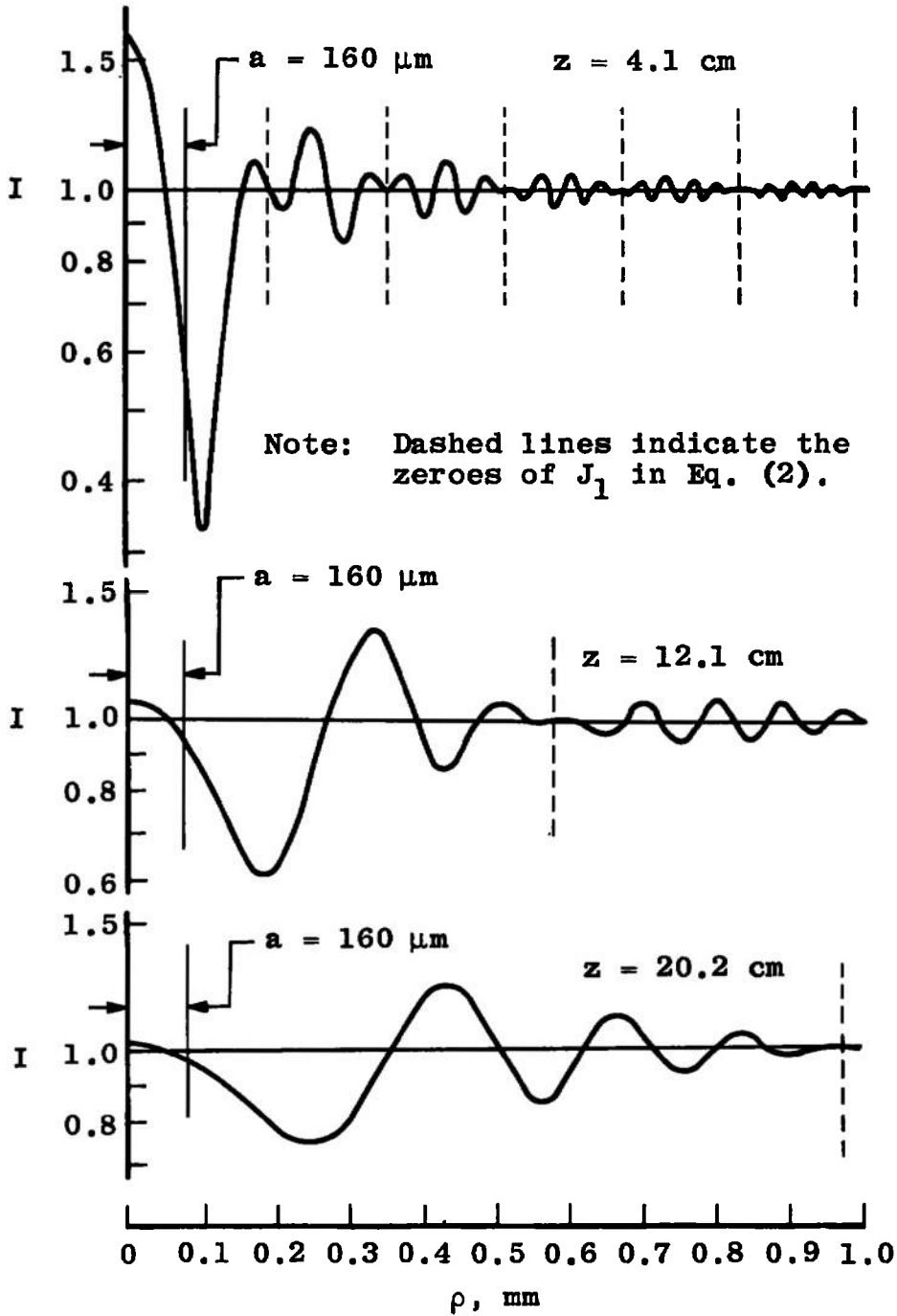
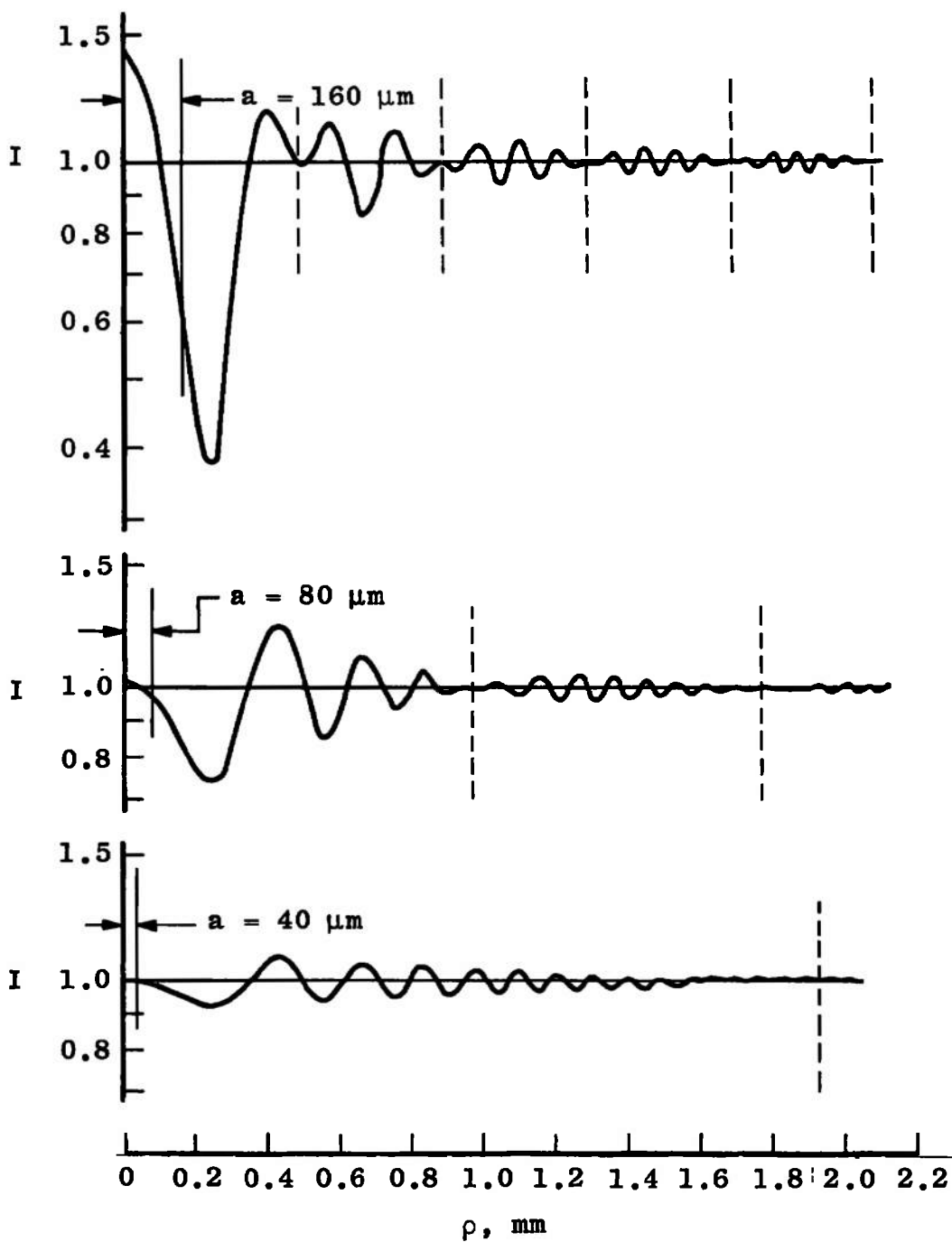


Fig. 9 Conjugate Image Overlap Recording Condition



a. Patterns of the Intensity,  $I$ , versus the Position Vector,  $\rho$ , for a Fixed Particle Diameter of  $160 \mu\text{m}$  and  $z = 4.1, 12.1$  and  $20.2 \text{ cm}$  with  $\lambda = 6328 \text{ \AA}$

Fig. 10 Theoretical Fraunhofer Diffraction Patterns



b. Patterns for  $z = 20 \text{ cm}$ ,  $\lambda = 6328 \text{ \AA}$ , and Particle Radii of 160, 80, and 40  $\mu\text{m}$ , Respectively  
 Fig. 10 Concluded



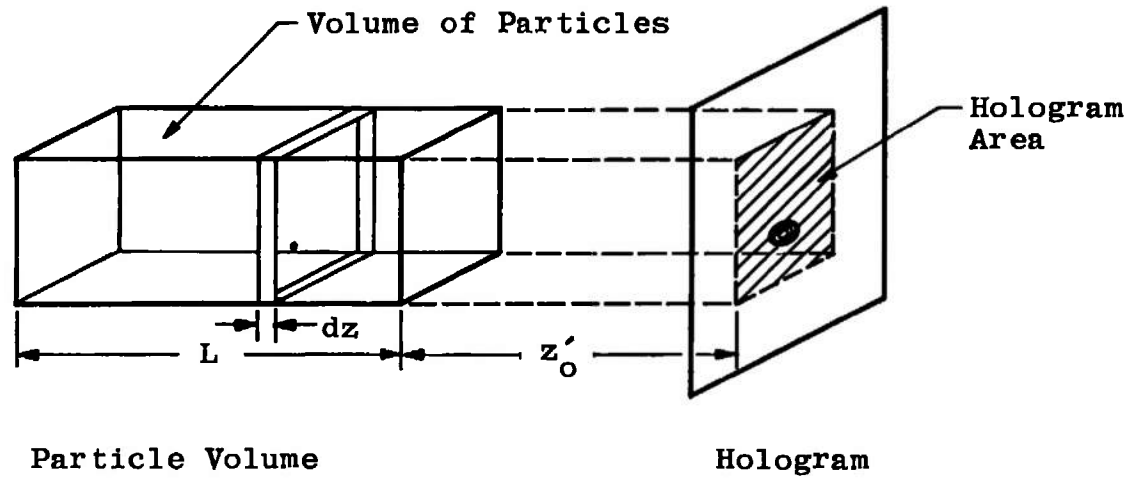


Fig. 11 Geometry of the Particle Number Density Derivation for Hologram Recordings

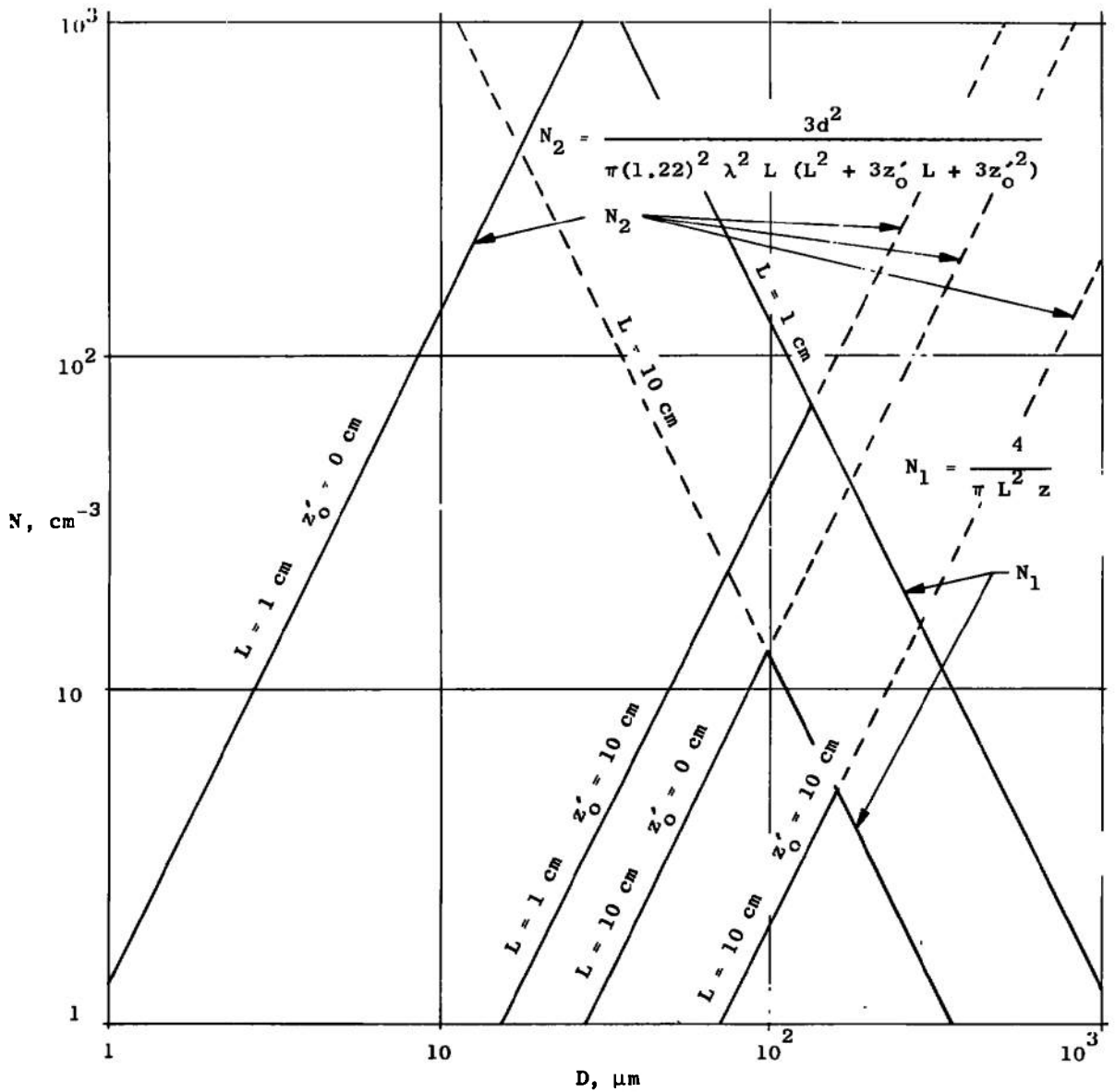
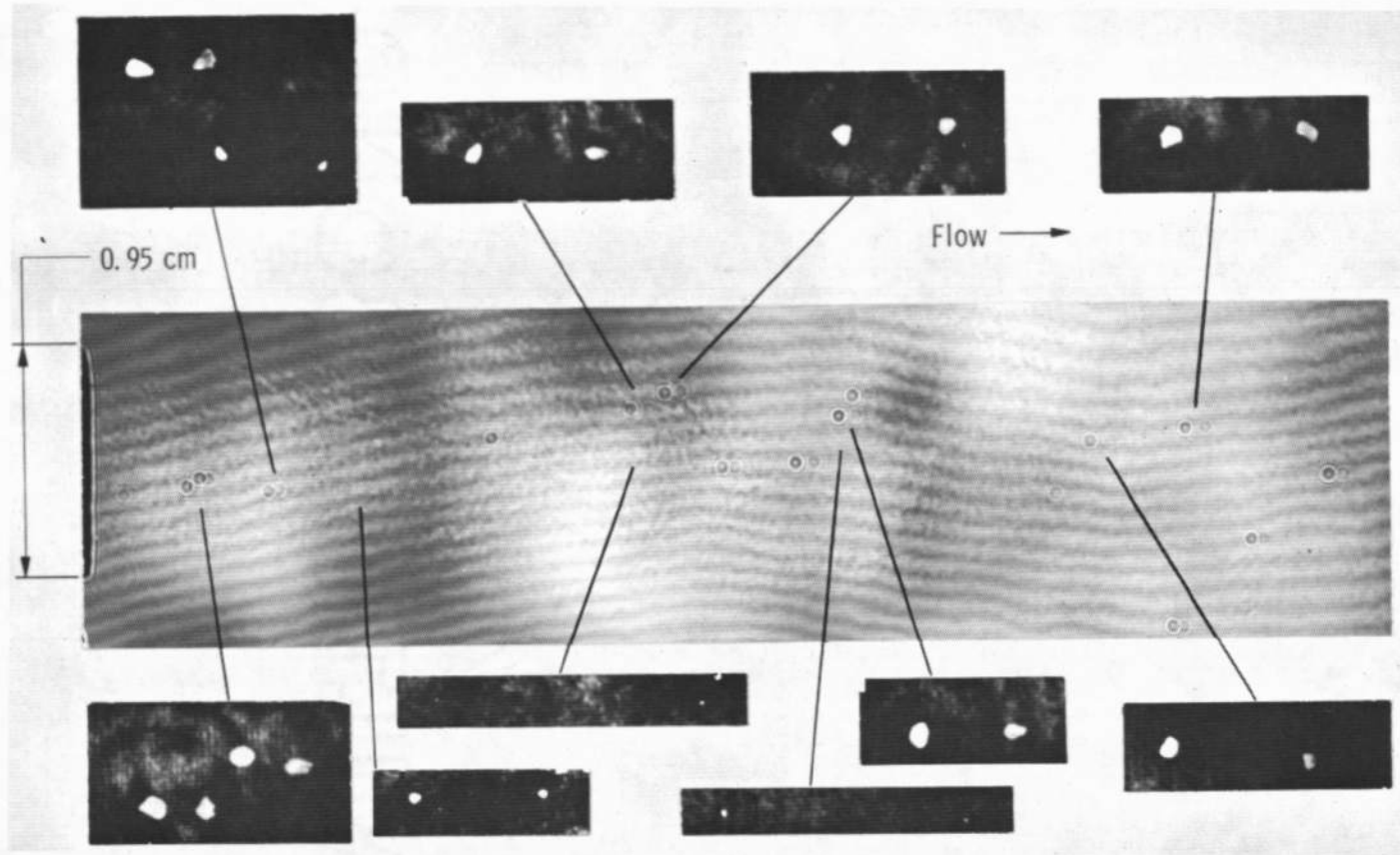


Fig. 12 Number Density versus Diameter for Marginal and No-Hologram Recordings



- Note: (1) Large Particles Are Nominal 100- $\mu$ m Diameter  
 (2) Magnification Is the Same for All Reconstructions Shown  
 (3) Pulse Separation - 12  $\mu$ sec  
 (4) Dust Material - MgO

**Fig. 13 Double-Pulsed Holography of a Moving Dust Field**

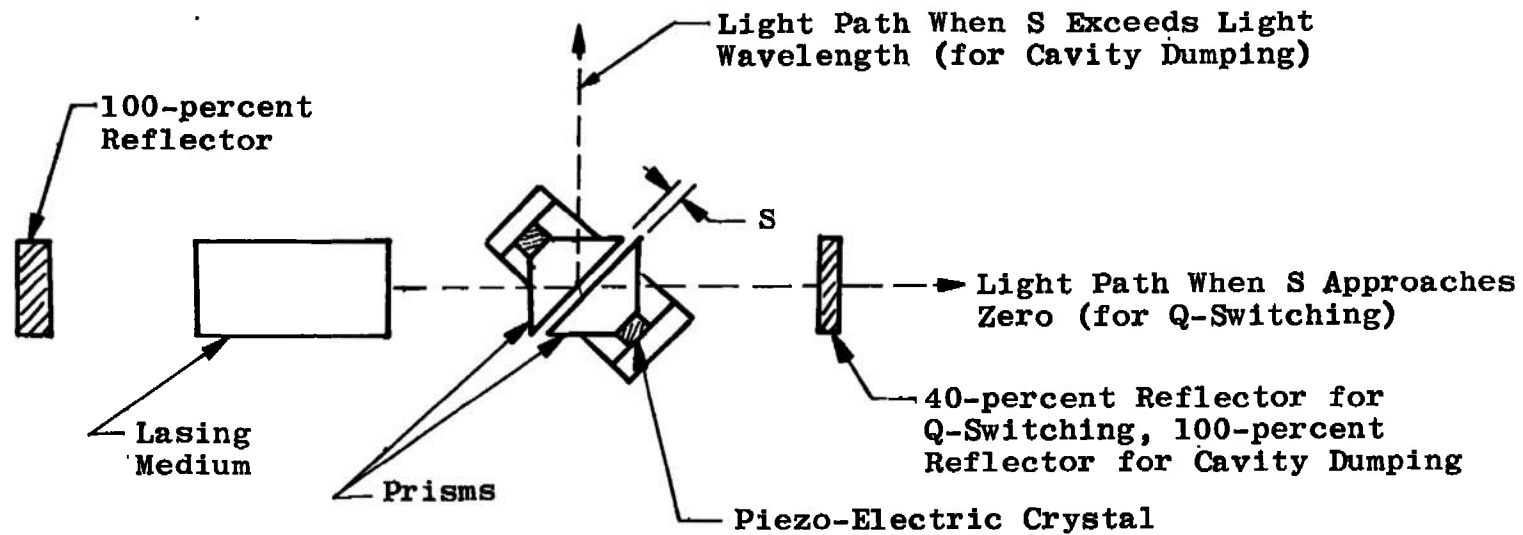


Fig. 14 Frustrated Internal Reflection Q-Switching

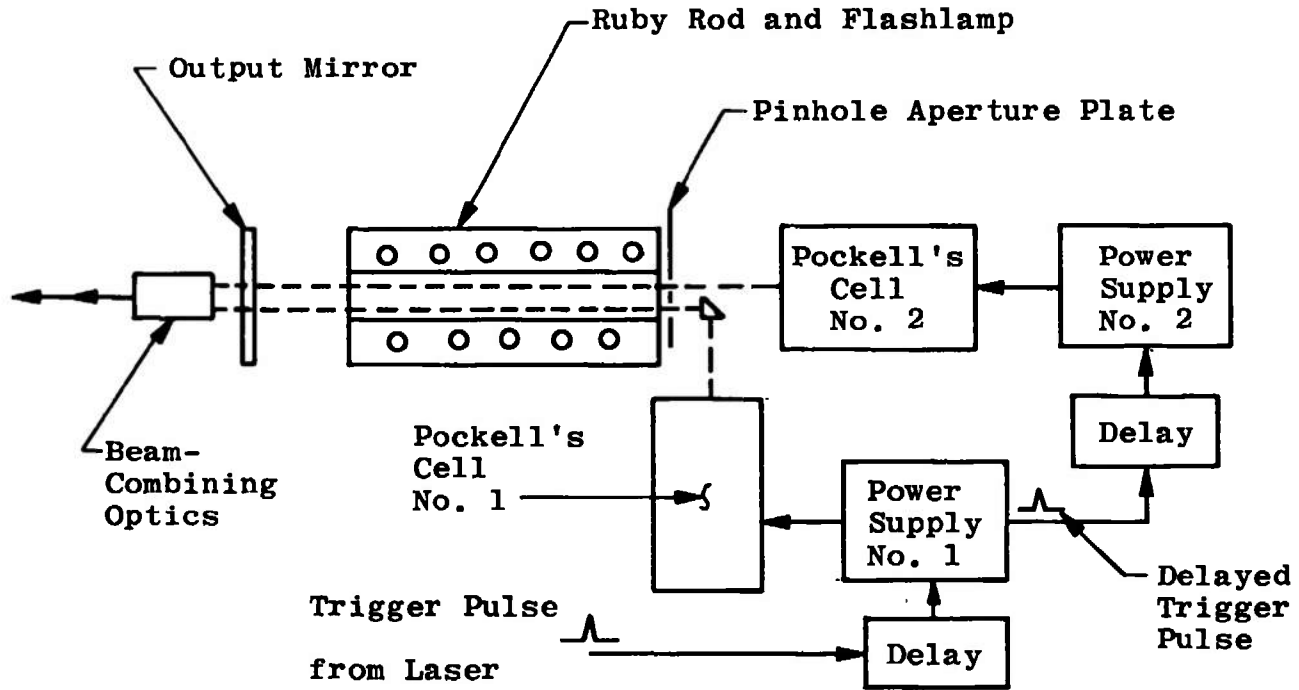


Fig. 15 Double-Barrelled, Double-Pulsing Laser Schematic

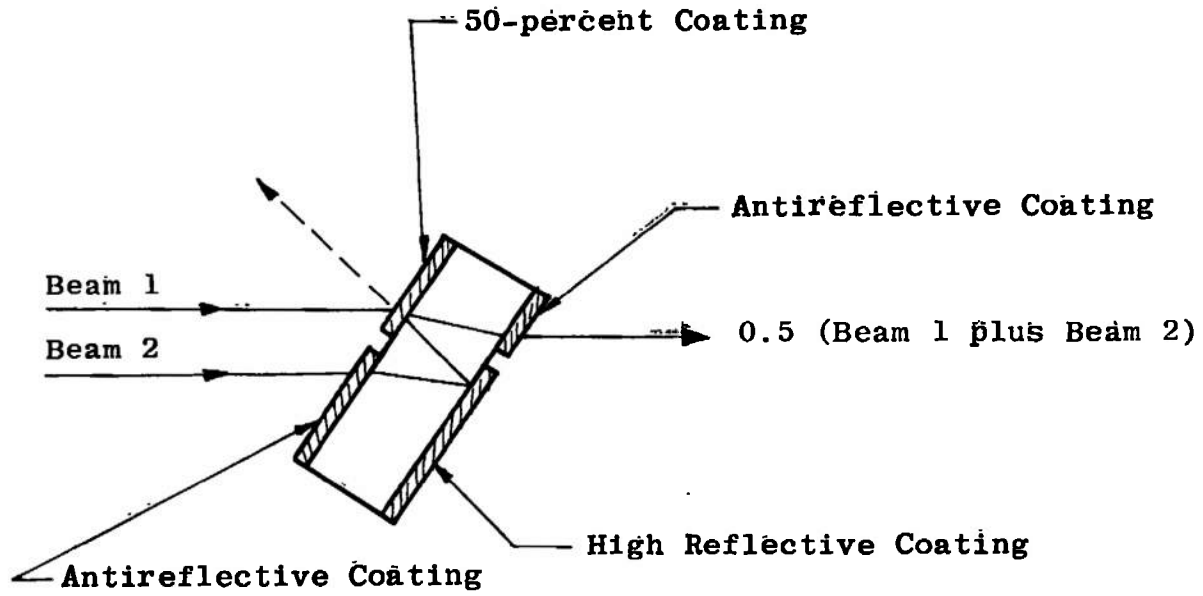


Fig. 16 Beam-Combining Optics

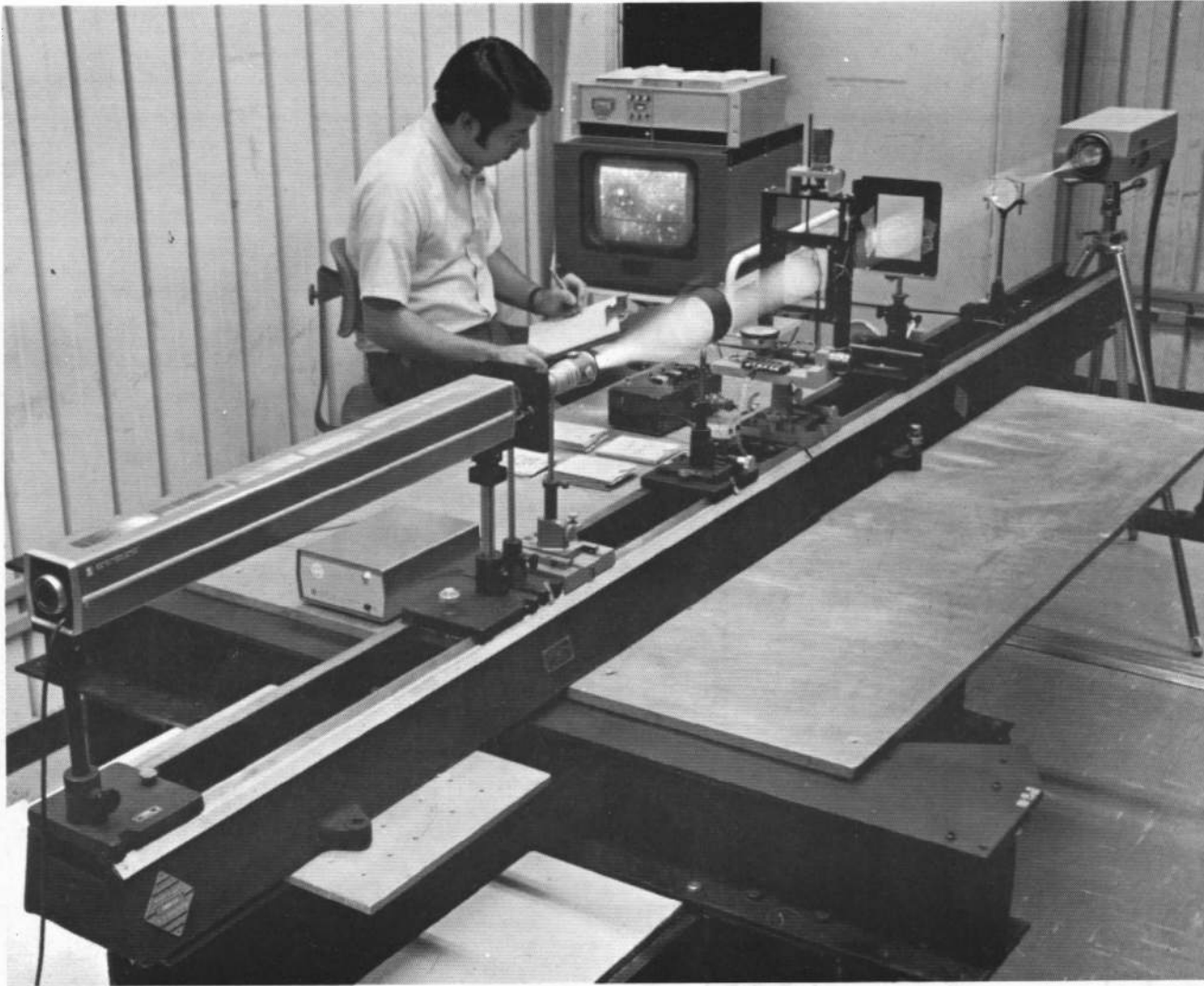
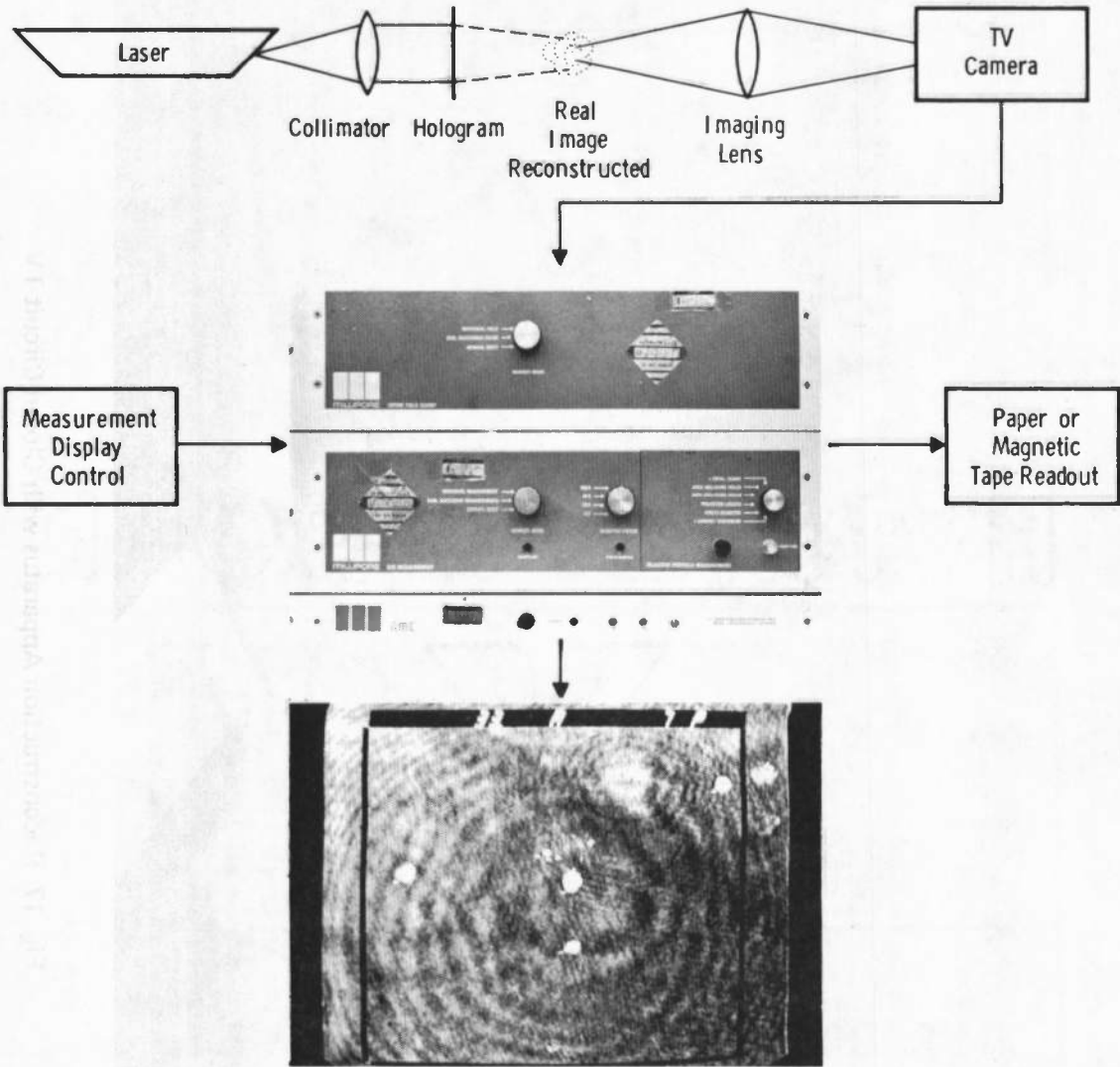
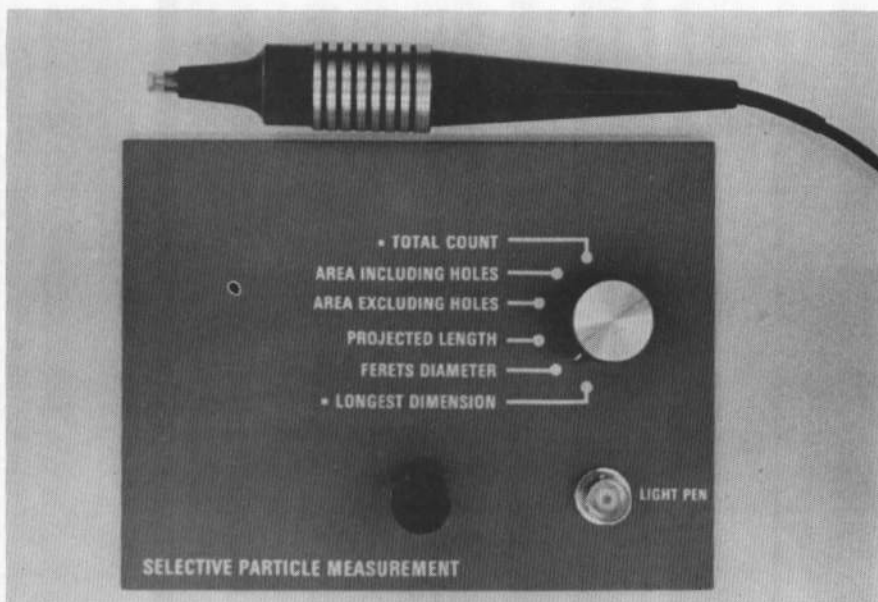


Fig. 17 Reconstruction Apparatus with Closed-Circuit TV

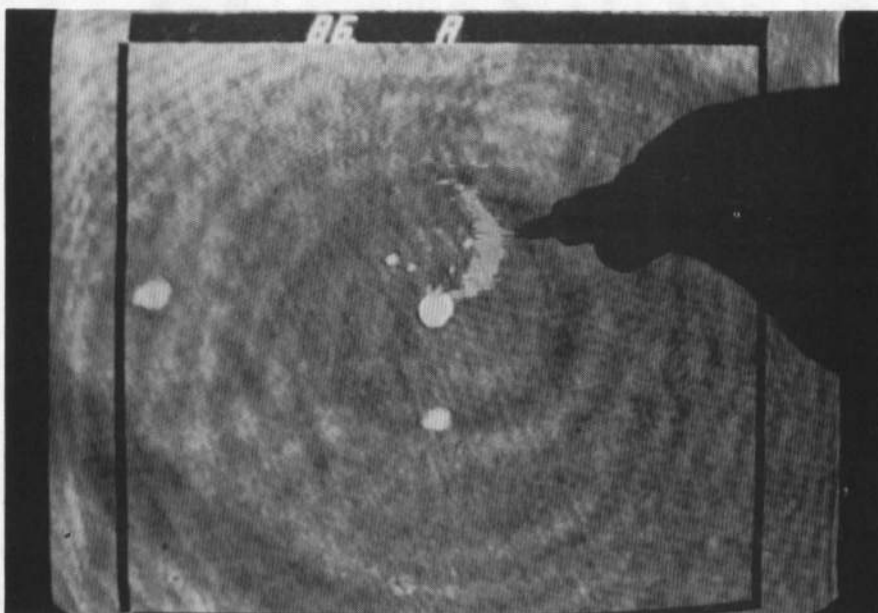


a. Reconstruction Setup with the Computerized Image Analyzer  
 Fig. 18 Computerized Image Analyzer





b. Light Pen and Individual Measurement Module



c. Light Pen in Use on CCTV Monitor  
Fig. 18 Concluded

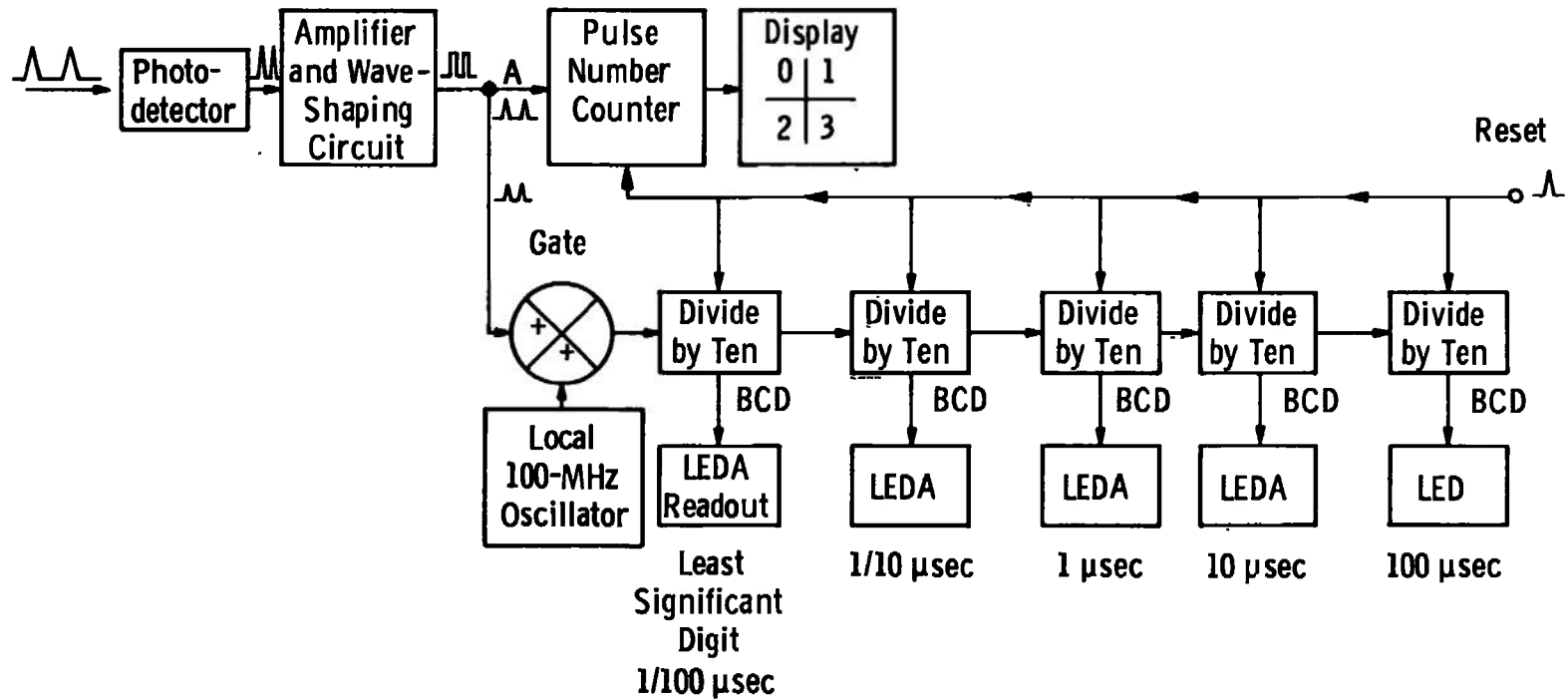


Fig. 19 Laser Light Pulse Interval Counter

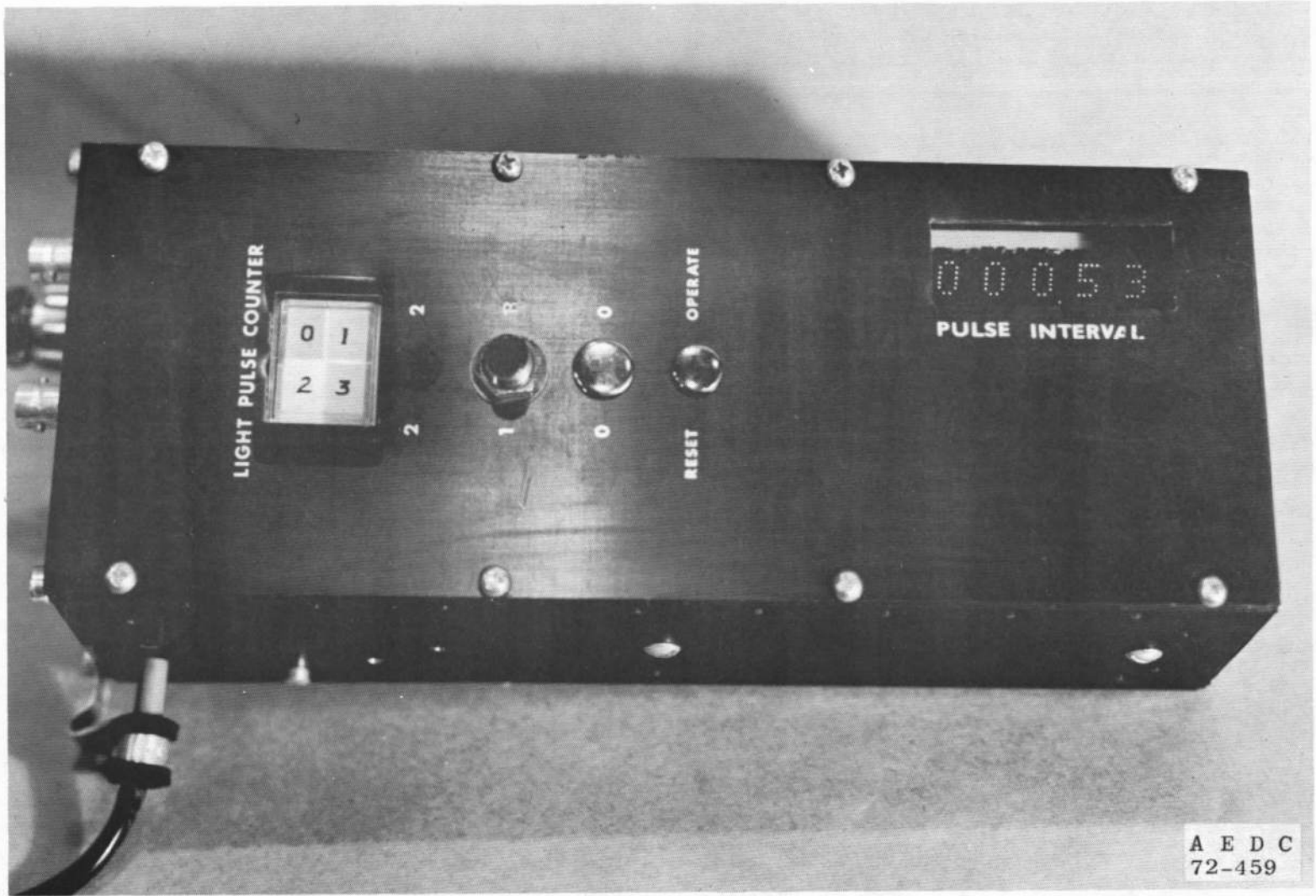


Fig. 20 Pulse Counter and Time Interval Counter

A E D C  
72-459

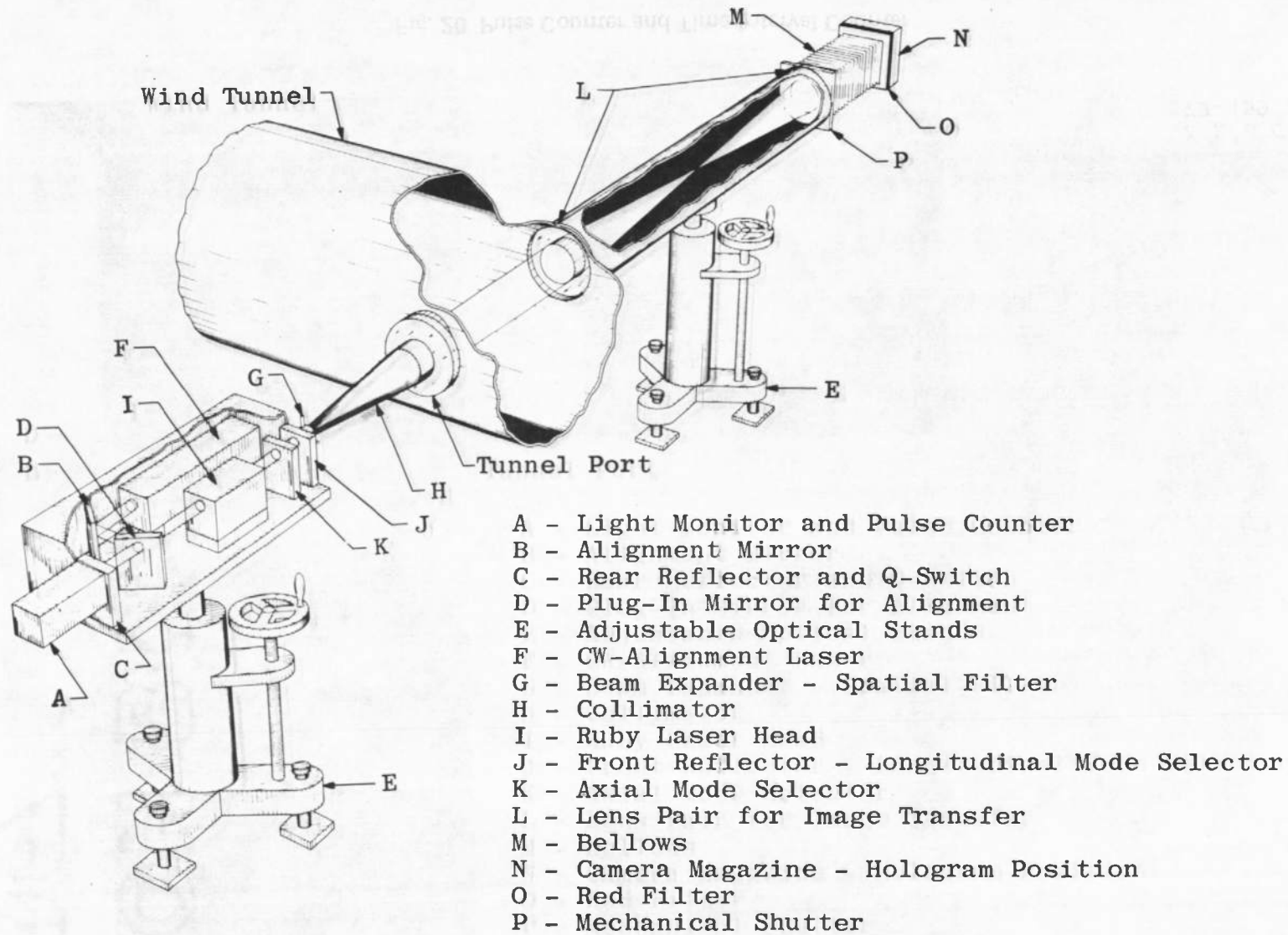
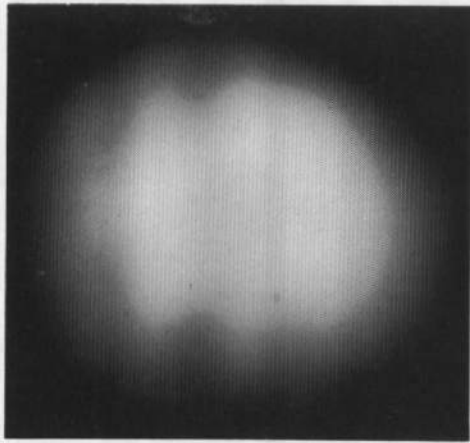
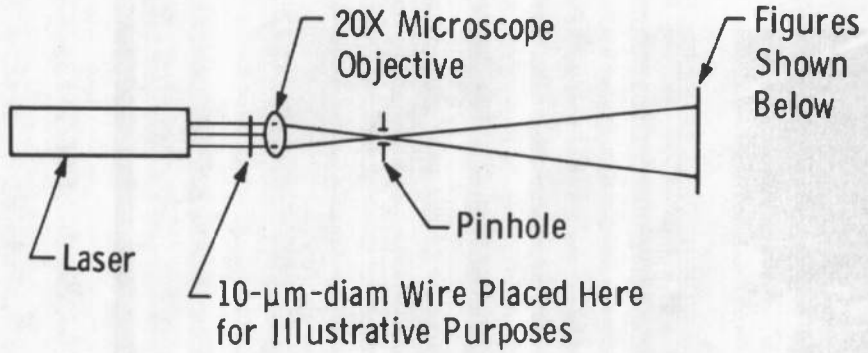
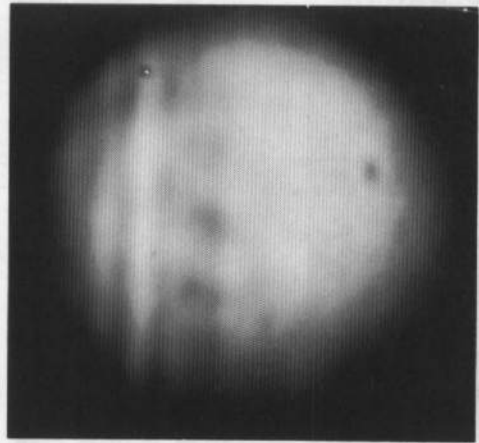


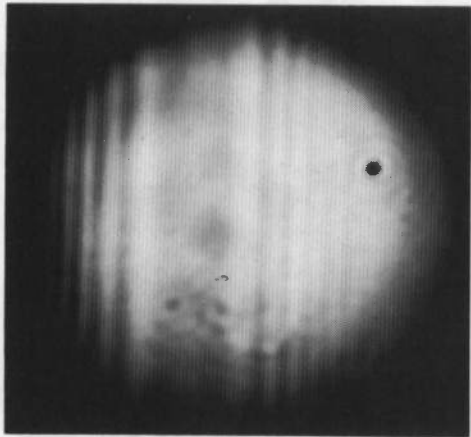
Fig. 21 In-Line Image Holocamera



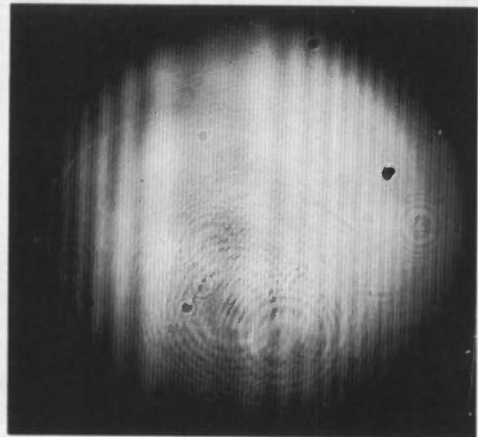
a.  $d = 30 \mu\text{m}$



b.  $d = 100 \mu\text{m}$



c.  $d = 200 \mu\text{m}$



d. Without Pinhole ( $d = \infty$ )

Fig. 22 Spatial Filtered Beams with Various Pinhole Sizes

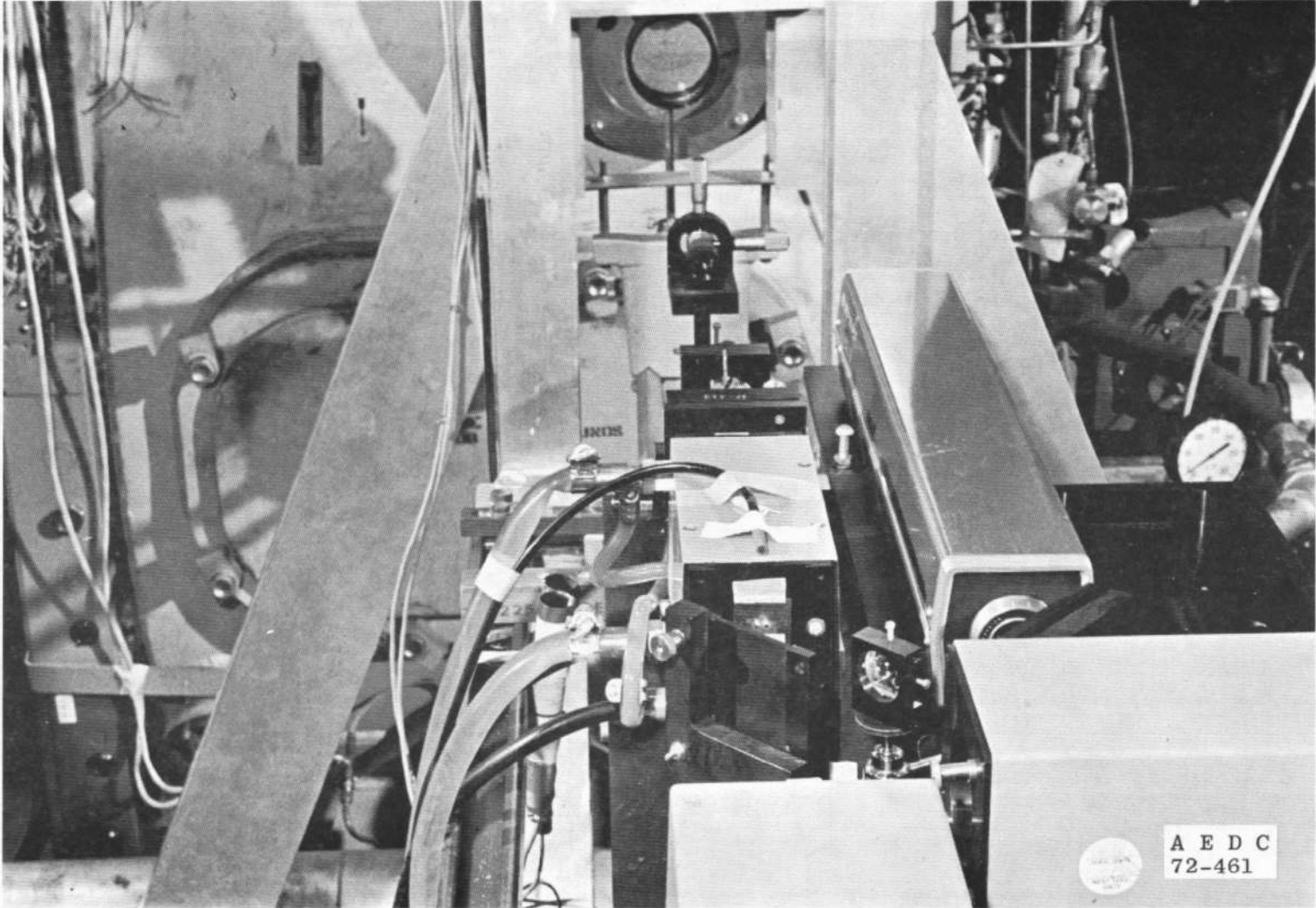


Fig. 23 Dust Erosion Facility Holocamera (Laser Side)



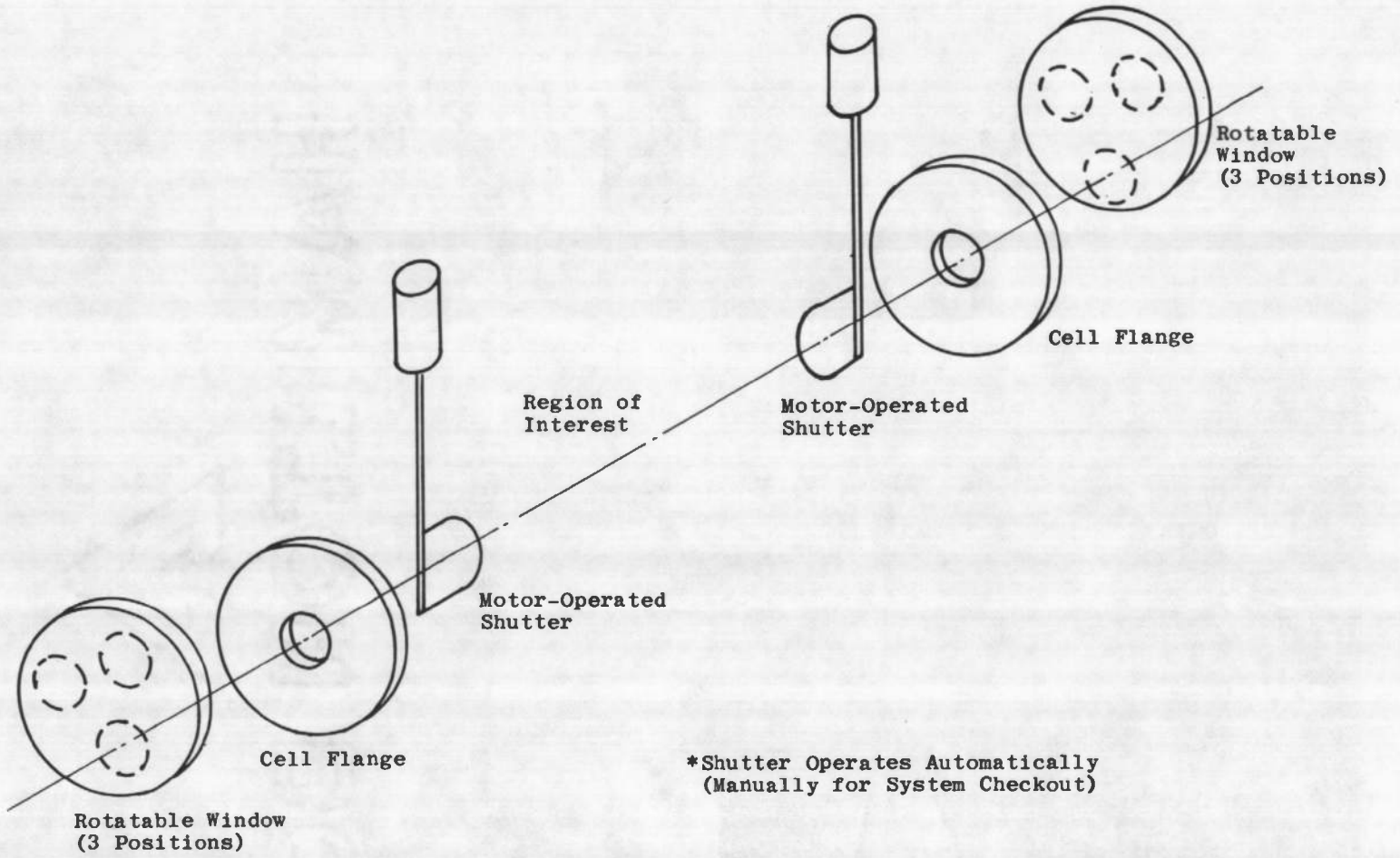


Fig. 24 Window Protection System

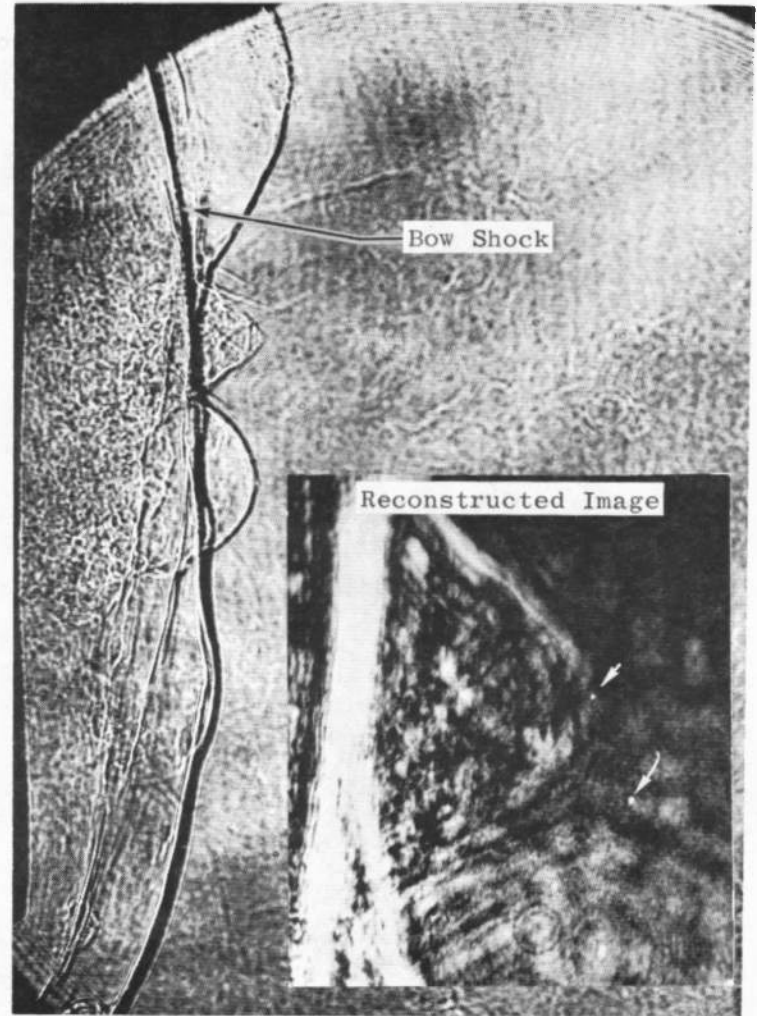
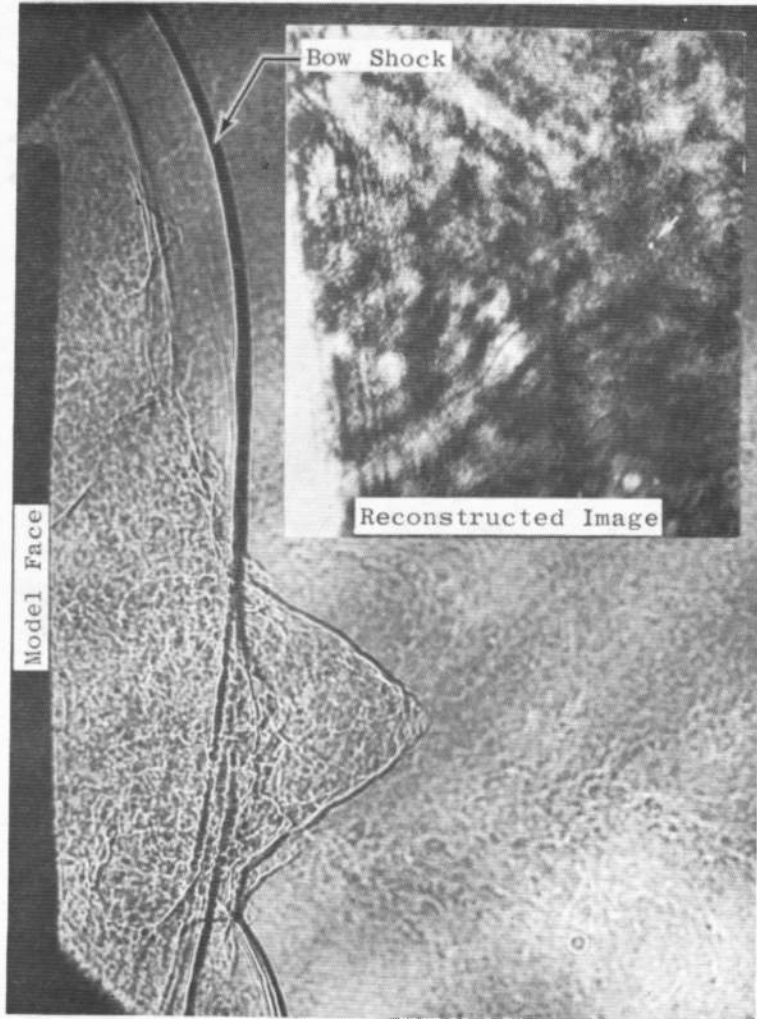


Fig. 25 Holograms and Images of Particles Penetrating the Bow Shock



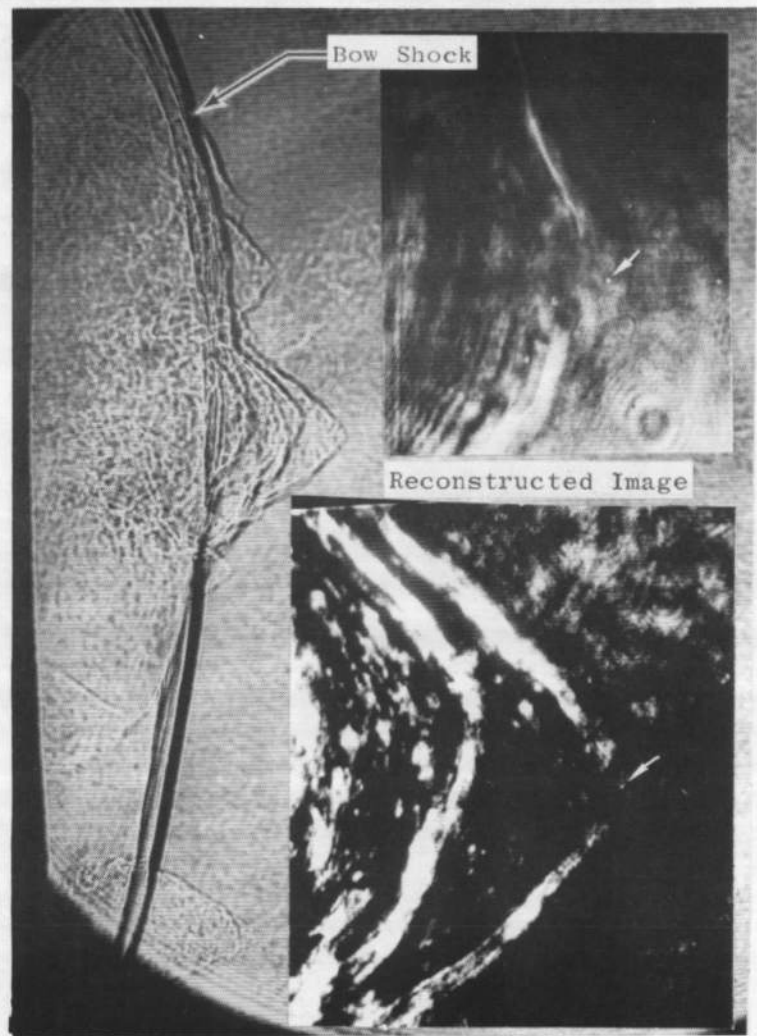
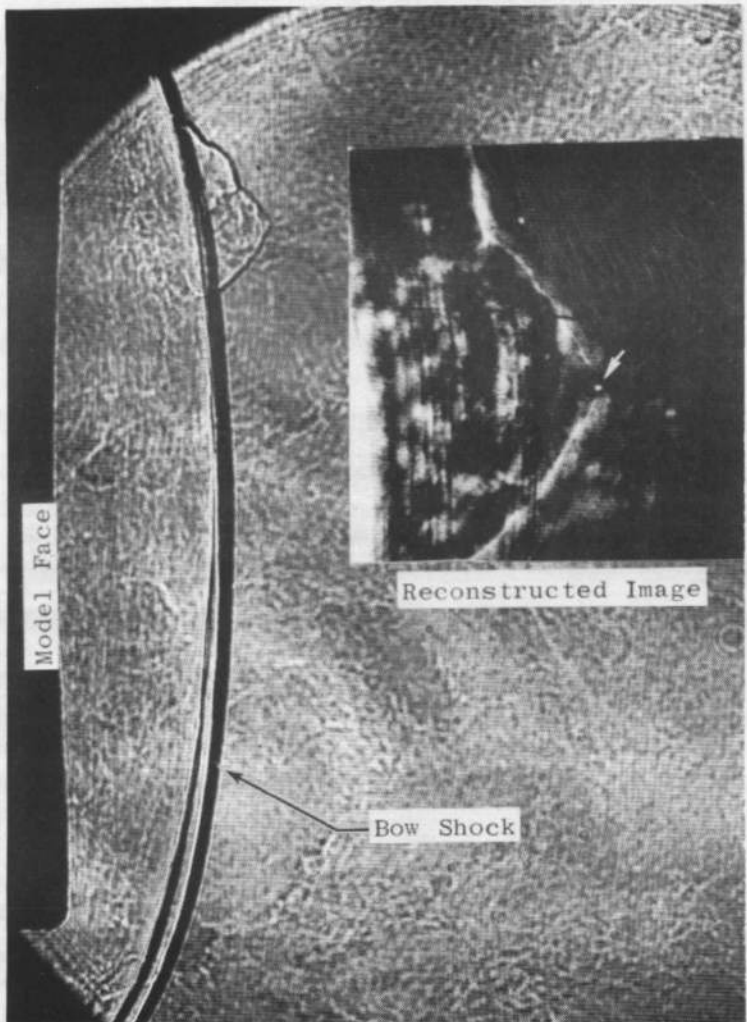


Fig. 25 Concluded

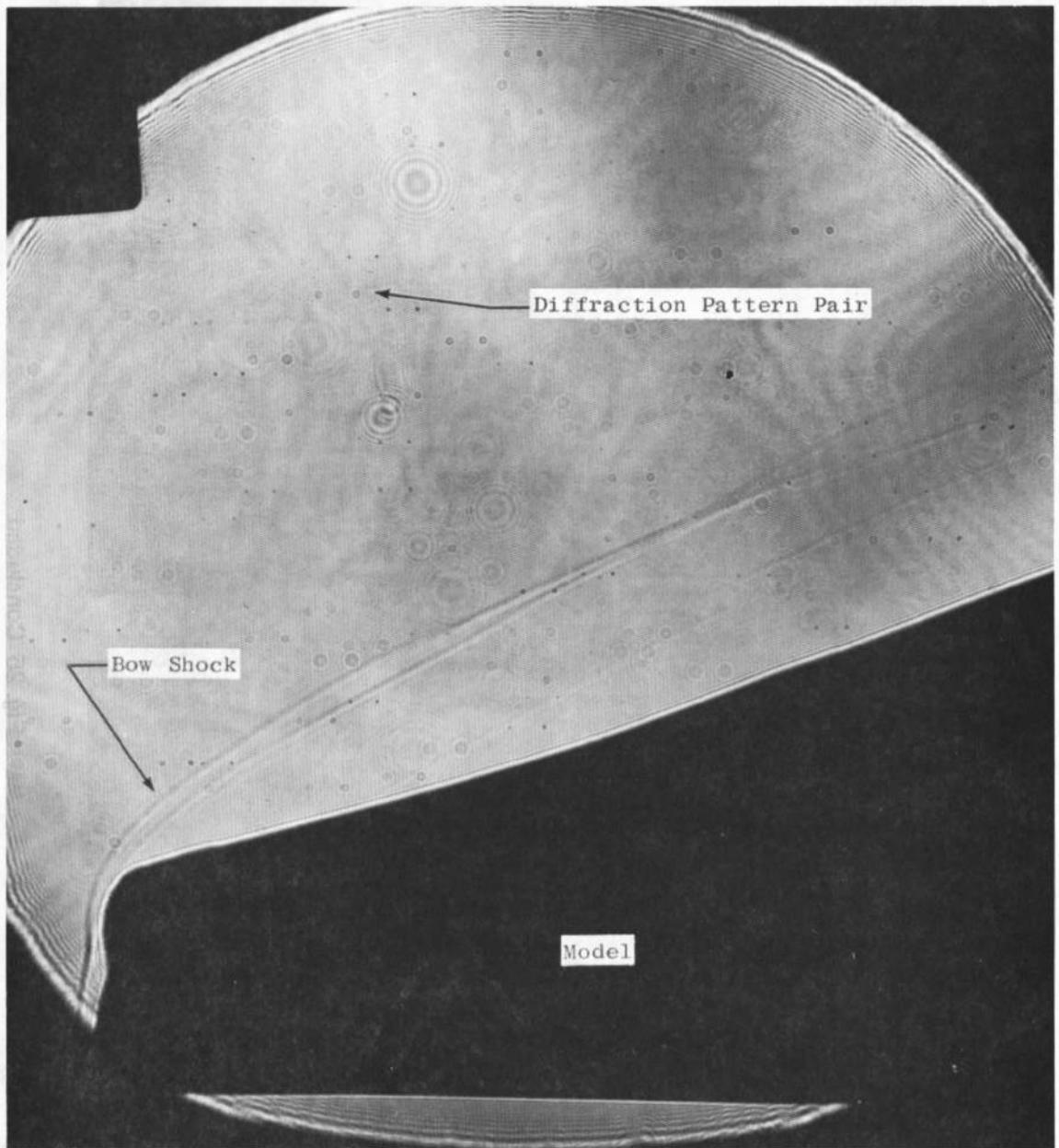
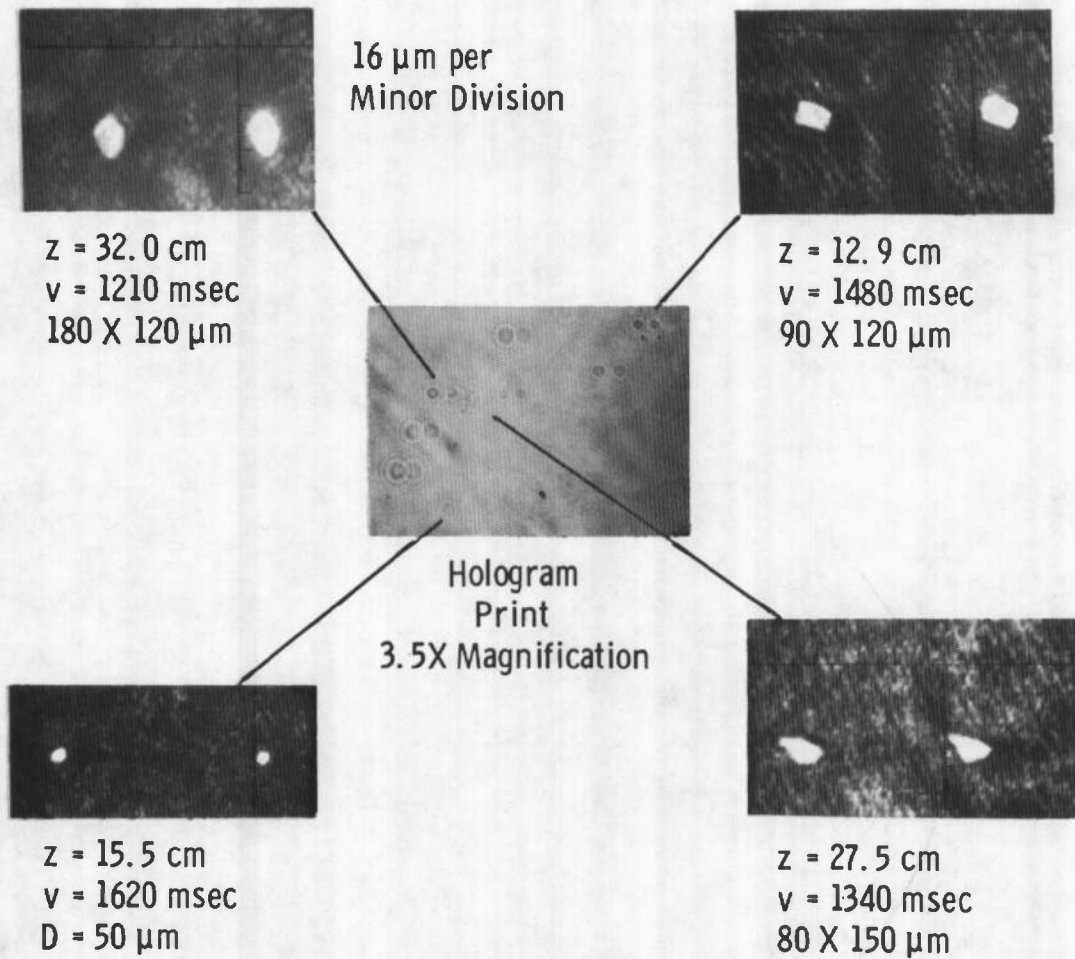


Fig. 26 Sample Hologram of Model in PWT Dust Erosion Facility



Note - Reconstructed Images Photographed  
from TV Monitor  
Pulse Separation =  $0.45 \mu\text{sec}$

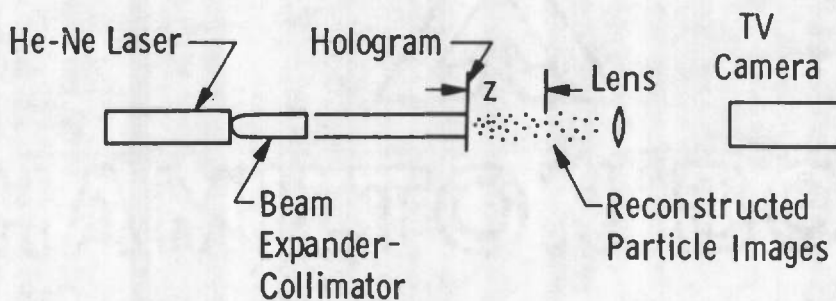


Fig. 27 Double-Exposure Hologram of a High-Speed Dust Field and Some Reconstructions

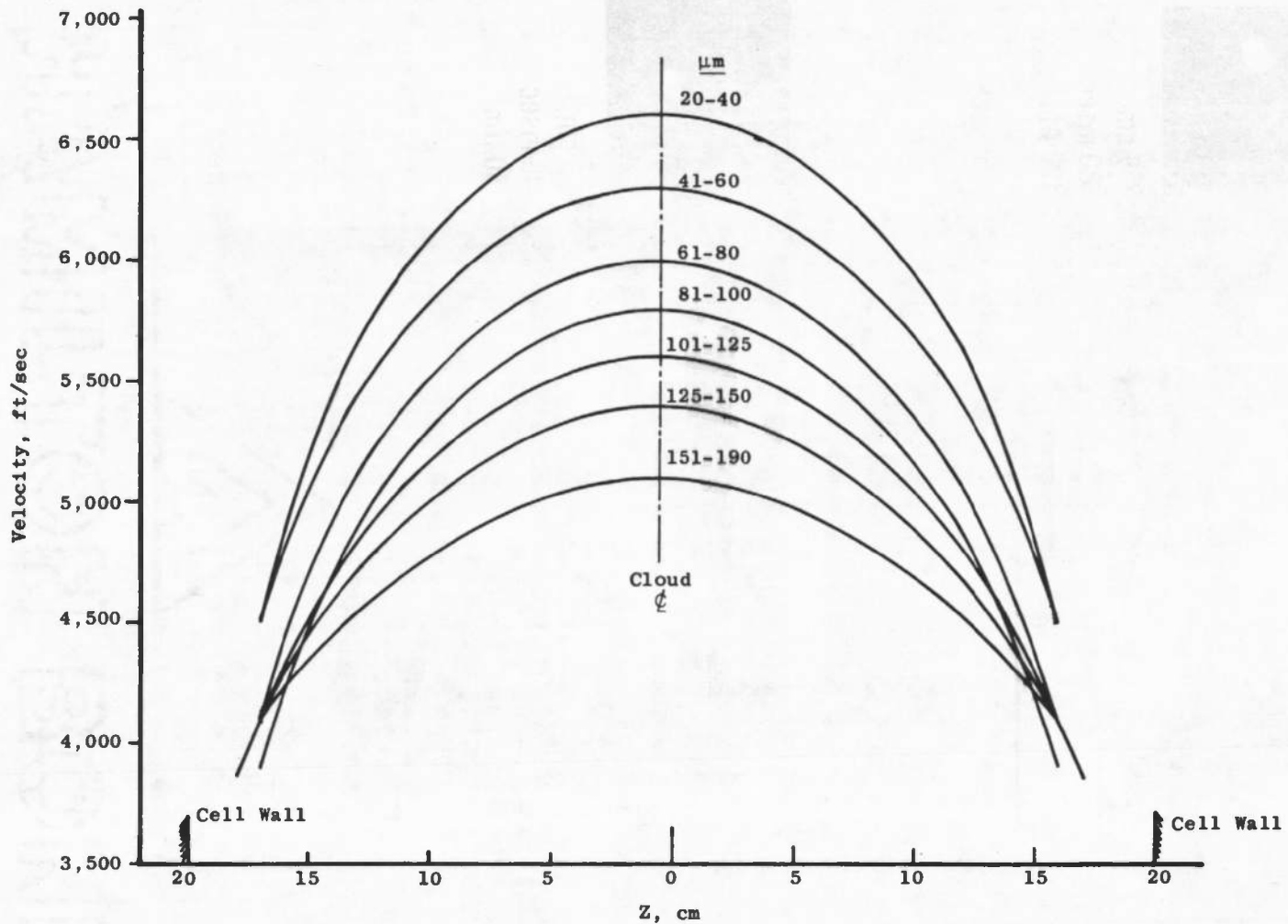


Fig. 28 Velocity Spatial Distribution Curves

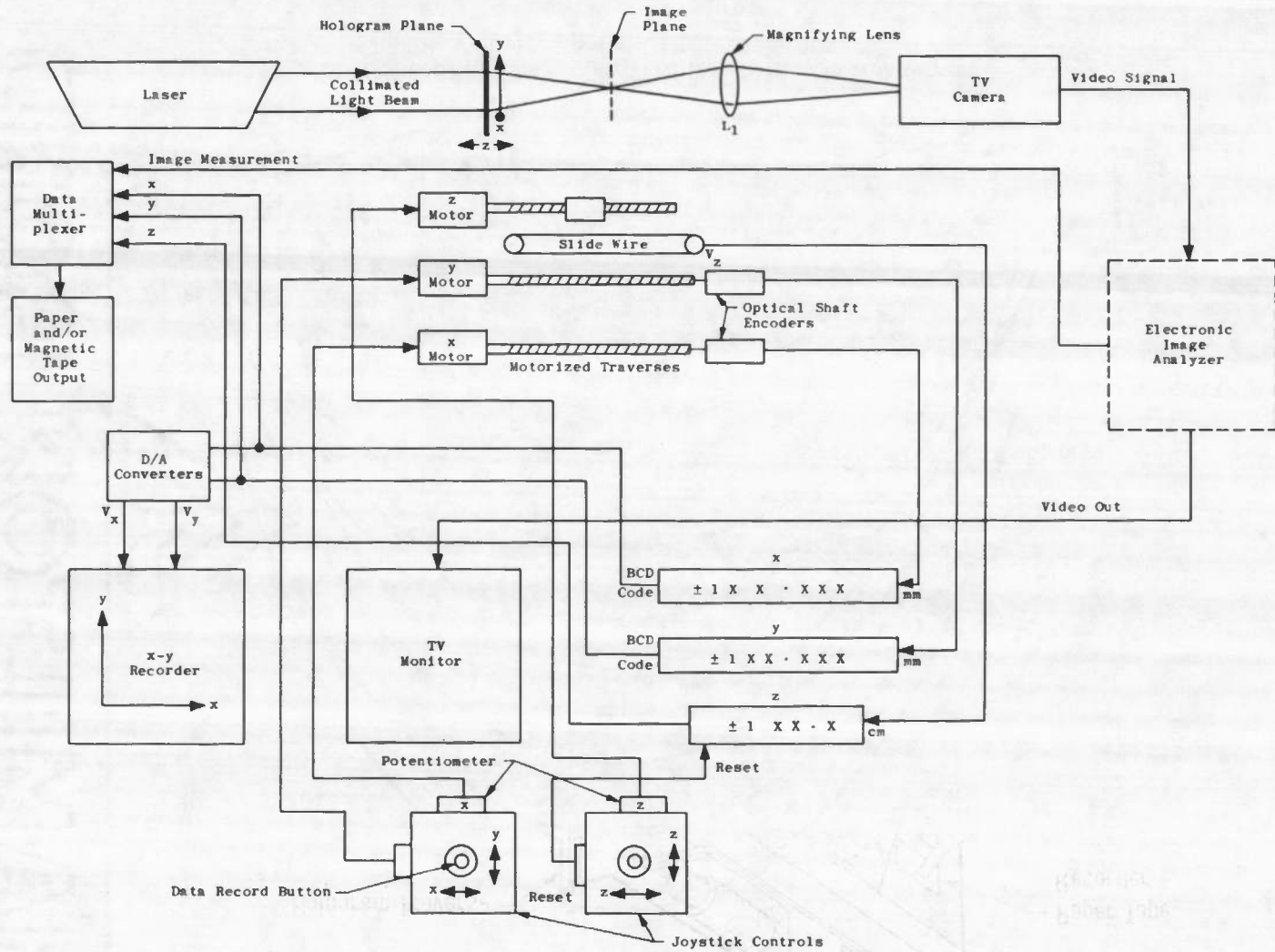


Fig. 29 Automated Hologram Analyzing System

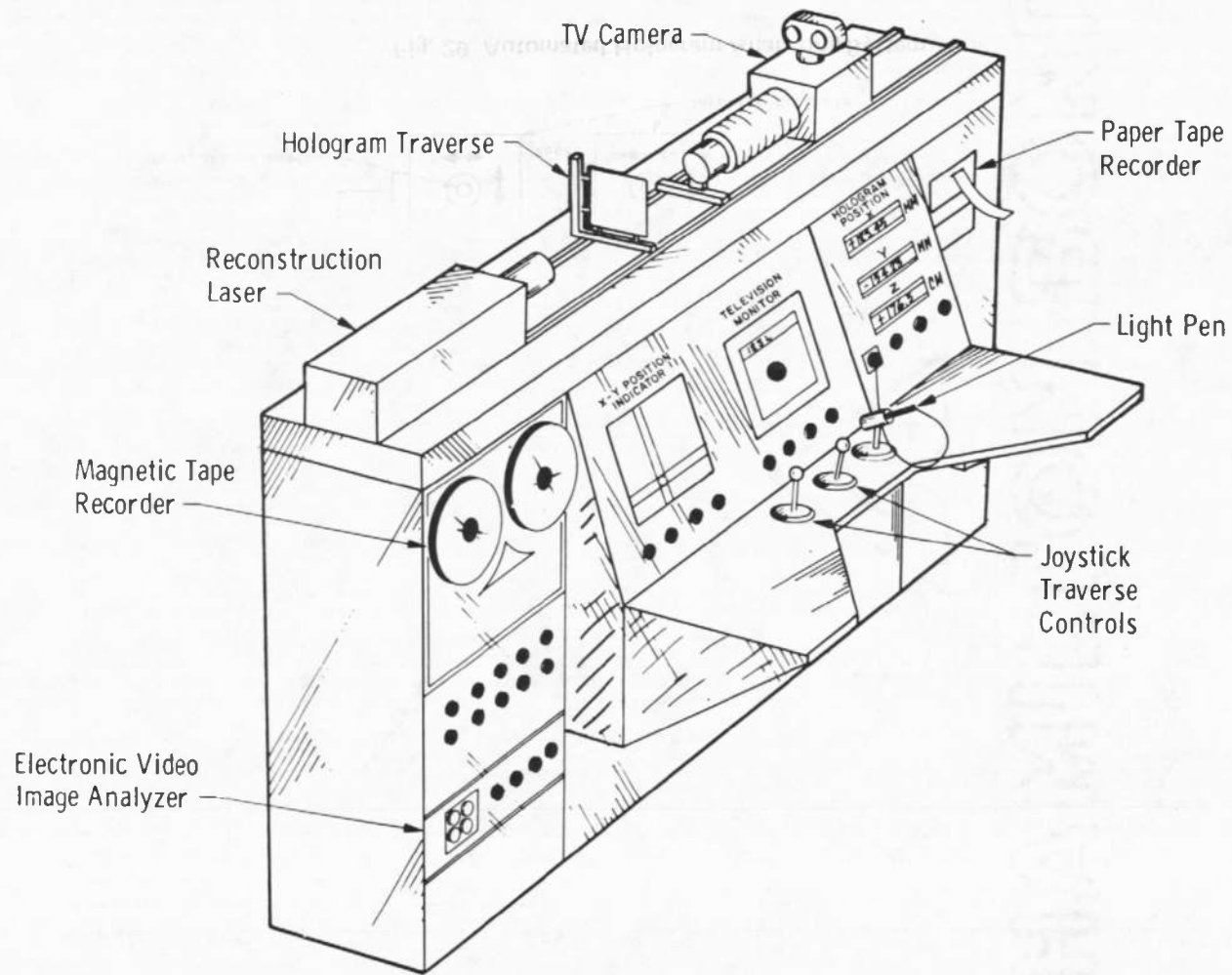


Fig. 30 Conceptual Drawing of Proposed Hologram Analyzer

UNCLASSIFIED

Security Classification

DOCUMENT CONTROL DATA - R & D

(Security classification of title, body of abstract and indexing annotation must be entered when the overall report is classified)

1 ORIGINATING ACTIVITY (Corporate author) Arnold Engineering Development Center Arnold Air Force Station, Tennessee 37389		2a. REPORT SECURITY CLASSIFICATION UNCLASSIFIED	
		2b. GROUP N/A	
3 REPORT TITLE HOLOGRAPHY IN DUST EROSION FACILITIES			
4 DESCRIPTIVE NOTES (Type of report and inclusive dates) Final Report -- July 1970 through June 1972			
5 AUTHOR(S) (First name, middle initial, last name) J. D. Trolinger and R. A. Belz, ARO, Inc.			
6 REPORT DATE September 1973		7a. TOTAL NO OF PAGES 72	7b. NO. OF REFS 14
8a. CONTRACT OR GRANT NO		9a. ORIGINATOR'S REPORT NUMBER(S) AEDC-TR-73-160	
b. PROJECT NO		9b. OTHER REPORT NO(S) (Any other numbers that may be assigned this report)	
c. Program Element 65802F		ARO-OMD-TR-72-168	
d.			
10 DISTRIBUTION STATEMENT Approved for public release; distribution unlimited.			
11 SUPPLEMENTARY NOTES Available in DDC.		12 SPONSORING MILITARY ACTIVITY Arnold Engineering Development Center, Air Force Systems Command, Arnold AF Station, Tennessee 37389	
13 ABSTRACT Extensive application of holographic techniques has been made in the ground test facilities at the Arnold Engineering Development Center (AEDC) for particle-field analysis and flow diagnostics. The instrumentation requirements of dust erosion facilities include a dynamic evaluation of the dust cloud, including size, number density, velocity, and distribution of dust particles. Holography has provided a unique method of performing such an evaluation. The system developed at AEDC and currently in routine use is discussed in detail. Design criteria and system capability are analyzed. It is shown that the holography system provides data which cannot be obtained with other existing instrumentation.  Approved for public release; distribution unlimited.			



14. KEY WORDS	LINK A		LINK B		LINK C	
	ROLE	WT	ROLE	WT	ROLE	WT
holograms lasers optical measurement diffraction dust particle size distribution flow distribution						

AFSC  
Area 4 AF1 Tech